Agglomeration and Defluidisation Behaviour of High-Sodium, High-Sulphur South Australian Lignite under Fluidised Bed Gasification Conditions

Daniel Peter McCullough

Thesis submitted for the degree of

Doctorate of Philosophy

School of Chemical Engineering

The University of Adelaide

January 2007

BIBLIOGRAPHY

Altwicker, E.R. and Konduri, R.K.N.V., "Hydrodynamic aspects of spouted beds at elevated temperatures," *Combust. Sci. and Tech.*, 87, 173-197 (1992).

ASTM, "Standard test method for fusibility of coal and coke ash," *Annual Book of ASTM Standards*, Designation: D 1857-87 (1994).

Anthony, E.J., Ross, G.G., Berry, E.E., Hemings, R.T., Kissel, R.K., and Doiron, C.C., "Characterization of solid wastes from CFBC," *Proceedings of the 10th International Conference on FBC*, 1, 131-139 (1989).

Apte, A.J. and Fein, H.L., "Application of controlled temperature carbonization to avoid coal agglomeration during gasification," *AIChE Symposium Series*, 77, 200-207 (1981).

Atakul, H. and Ekinci, E., "Agglomeration of Turkish lignites in fluidised-bed combustion," *J. Inst. Energy*, March, 56-61 (1989).

Attar, A., "Chemistry, thermodynamics and kinetics of reactions of sulphur in coal-gas reactions: A review," *Fuel*, 57(4), 201-212 (1978).

Attar, A. and Dupuis, F., "Data on the distribution of organic sulfur functional groups in coals," *Advances in Chemistry Series*, 192, 239-256 (1981).

Barnhart, D.H. and Williams, P.C., "The Sintering Test, an index to ash-fouling tendency," *Trans. ASME*, 78, 1229-1236 (1956).

Basu, P., "A study of agglomeration of coal-ash in fluidized beds," *The Canadian Journal of Chemical Engineering*, 60, 791-795 (1982).

Basu, P. and Sarka, A., "Agglomeration of coal ash in fluidized beds," *Fuel*, 62, 924-926 (1983).

Beaupeurt, I., "PDU (Pressurised Development Unit) Gasifier – Commissioning and Operational Capability," *Proceedings of Eighth Annual Conference, CRC for Clean Power from Lignite*, 107- 112 (2001).

Beaupeurt, I., Bhattacharya, S. and Donnan, T., "Gasifier PDU (Process Development Unit) – Plant operation overview," *Proceedings of Ninth Annual Conference, CRC for Clean Power from Lignite*, 25-30 (2002).

Beaupeurt, I., Topping, B. and Bhattacharya, S., "Gasifier PDU: Activities in 2003-04," *Proceedings of Eleventh Annual Conference, CRC for Clean Power from Lignite*, 37-42 (2004).

Benson, S.A., Sondreal, E.A. and Hurley, J.P., "Status of coal ash behavior research," *Fuel Processing Technology*, 44, 1-12 (1995).

Berner, *J. Geology*, 72, 293 (1964).

Bhattacharya, S.P., "Gasifier PDU: Activities in 2004-05," *Proceedings of Twelfth Annual Conference, CRC for Clean Power from Lignite*, 29-34 (2005a).

Bhattacharya, S.P., *Personal Communication*, (2005b).

Bhattacharya, S.P., "Preliminary results from fluidized bed gasification of Victorian brown coal," *Proceedings of Fourth Annual Conference, CRC for Clean Power from Lignite*, 15-19 (1997).

Bhattacharya, S.P., Beaupeurt, I. and Donnan, T., "Test program using the gasifier PDU: Preliminary results and their implications," *Proceedings of Ninth Annual Conference, CRC for Clean Power from Lignite*, 19-24 (2002).

Bhattacharya, S., Kosminski, A., Yan, H., Vuthaluru, H. and Wirawan, A., "Combustion of Victorian and South Australian low-rank coals in a circulating fluidised bed combustion pilot plant," *CRC for Clean Power from Lignite*, Internal Report No. 99014, (1999).

Bridgwater, J., "Spouted beds," in *Fluidization*, 2nd edition, edited by Davidson, J.F., Clift, R. and Harrison, D., Academic Press (1985), Chapter 6.

Brinsmead, K.H. and Kear, R.W., "Behaviour of sodium chloride during the combustion of carbon," *Fuel*, 35, 84-93 (1956).

Brockway, D.J., Ottrey, A.L. and Higgins, R.S., "Chapter 11: Inorganic constituents," in *The Science of Victorian Brown Coals: Structure, Properties and Consequences for Utilization*, edited by Durie, R.A., Butterworth-Heinemann (1991), 597-650.

Brown, H.R. and Swaine, D.J., "Inorganic constituents of Australian coals: Part I. Nature and mode of occurrence," *J. Inst. Fuel*, 37, 422-434 (1964).

Burns, M.S., Durie, R.A. and Swaine, D.J., "Significance of chemical evidence for the presence of carbonate minerals in brown coals and lignites," *Fuel*, 41, 373-383 (1962).

Calkins, W.H., "Determination of organic sulfur-containing structures in coal by flash pyrolysis experiments," *Preprints of Papers - American Chemical Society, Division of Fuel Chemistry*, 30(4), 450-465 (1985).

Calkins, W.H., "The chemical forms of sulfur in coal: a review," *Fuel*, 73(4), 475-484 (1994).

CSIRO, "Determination of carboxyl groups in low-rank coals," *Coal Research in CSIRO*, n43, 7-8 (1971).

CSIRO, "Gasification of coal in fluidized beds," *Coal Research in CSIRO*, n37, 2-6 (1969).

Dawson, M.R. and Brown, R.C., "Bed material cohesion and loss of fluidization during fluidized bed combustion of midwestern coal," *Fuel*, 71, 585-592 (1992).

Dixon, K., Skipsey, E. and Watts, J.T., "The distribution and composition of inorganic matter in British coals: Part 1. – Initial study of seams from the East Midlands division of the National Coal Board," *J. Inst. Fuel*, 37, 485-493 (1964).

Dorin, H., "Chemistry: The study of matter," Needham, Massachusetts: Prentice Hall (1992), 674.

Durie, R.A., "The inorganic constituents in Australian coals III. Morwell and Yallourn brown coals," *Fuel*, 40, 407-422 (1961).

Durie, R.A and Swaine, D.J., "Inorganic constituents in coal," *Coal Research in CSIRO*, n45, 9-19 (1971).

Edgcombe, L.J., "State of combination of chlorine in coal I-Extraction of coal with water," *Fuel*, 35, 38-48 (1956).

Eglinton, M.S., "Concrete and its chemical behaviour," London: T. Telford (1987), 136p.

Ergudenler, A. and Ghaly, A.E., "Agglomeration of alumina sand in a fluidized bed straw gasifier at elevated temperatures," *Bioresource Technology*, 43, 259-268 (1993a).

Ergudenler, A. and Ghaly, A.E., "Agglomeration of silica sand in a fluidized bed gasifier operating on wheat straw," *Biomass and Bioenergy*, 4, 135-147 (1993b).

ETSA, "South Australian coalfields," *ETSA Report*, July (1988).

Favas, G. and Chaffee, A.L., "Mechanical Thermal Expression (MTE) – The first step in reducing Greenhouse Gas emissions from lignite power generation," *Proceedings of Eighth Annual Conference*, *CRC for Clean Power from Lignite*, 29-34 (2001).

Favas, G. and Chaffee, A.L., "The next generation of high quality brown coal fuels developed by using Mechanical Thermal Expression technology," *Proceedings of Seventh Annual Conference, CRC for Clean Power from Lignite*, 125-130 (2000).

Federer, J.I. and Lauf, R.J., "Crystallization behavior of coal gasification ash," *Nuclear and Chemical Waste Management*, 5, 221-229 (1985).

Foong, S.K., Cheng, G., and Watkinson, A.P., "Spouted bed gasification of Western Canadian coals," *The Canadian Journal of Chemical Engineering*, 59, 625-630 (1981).

Foong, S.K., Lim, C.J. and Watkinson, A.P., "Coal gasification in a spouted bed," *The Canadian Journal of Chemical Engineering*, 58, 84-91 (1980).

Francis, W., *Coal: Its Formation and Composition*, 2nd edition, Edward Arnold (Publishers) Ltd (1961), Chapter 1.

Geldart, D., "Types of gas fluidization," *Powder Technology*, 7, 285-292 (1973).

Geldart, D., Harnby, N. and Wong, A.C., "Fluidization of cohesive powders," *Powder Technology*, 37, 25-37 (1984).

Gloe, C.S. and Holdgate, G.R., "Chapter 1: Geology and resources," in *The Science of Victorian Brown Coals: Structure, Properties and Consequences for Utilization*, edited by Durie, R.A., Butterworth-Heinemann (1991), 1-43.

Gluckman, M.J., Yerushalmi, J. and Squires, A.M., "Defluidization characteristics of sticky or agglomerating beds," *Proc. of the Int. Fluidization Conf.*, California, USA, 15th-20th June (1975), 395-422.

Gluskoter, H.J., Shimp, N.F. and Ruch, R.R., "Chapter 7: Coal analyses, trace elements and mineral matter," in *Chemistry of Coal Utilization, Second Supplementary Volume*, edited by Elliot, M.A., Wiley-Interscience (1981), 369-424.

Gransden, J.F., Sheasby, J.S. and Bergougnou, M.A., "An investigation of defluidization of iron ore during reduction by hydrogen in a fluidized bed," *Chem. Eng. Prog. Symp. Series*, 66(105), 208-214 (1970).

Grant, K. and Weymouth, J.H., "The relationship of the inorganic constituents of Victorian brown coals to the fouling properties of the coals," *J. Inst. Fuel*, 35, 444-448 (1962).

Hall, F.P., Insley, H., "Phase diagrams for ceramists," American Ceramic Society, 152p (1947).

Halstead, W.D. and Raask, E., "The behaviour of sulphur and chlorine compounds in pulverized-coal-fired boilers," *Journal of the Institute of Fuel*, 42, 344-349 (1969).

He, Y., "Characterisation of spouting behaviour of coal ash with thermo-mechanical analysis," *Fuel Processing Technology*, 60, 69-79 (1999).

He, Y., "Particle agglomeration and loss of fluidisation in fluidised bed combustion," *CRC for Clean Power from Lignite*, Internal Report No. 98002 (1998).

He, Y., "Review on particle agglomeration and defluidisation in fluidised bed systems, Part I – Experimental," *CRC for Clean Power From Lignite*, Internal Report No. 96008 (1996).

Hodges, N.J., Ladner, W.R. and Martin, T.G., "Chlorine in coal: A review of its origin and mode of occurrence," *J. Inst. Energy*, 56, 158-169 (1983).

Hodges, N.J. and Richards, D.G., "The fate of chlorine, sulphur, sodium, potassium, calcium and magnesium during the fluidised bed combustion of coal," *Fuel*, 68, 440-445 (1989).

Hsieh, C.R. and Roberts, P.T., "A laboratory study of agglomeration in coal gasification," *Preprints American Chemical Society*, 30(3), 468-479 (1985).

Huffman, G.P., Huggins, F.E. and Dunmyre, G.R., "Investigation of the high-temperature behaviour of coal ash in reducing and oxidizing atmospheres," *Fuel*, 60, 585-597 (1981).

Huynh, D., "Review and development of lignite dewatering process for power generation," *Proceedings of Seventh Annual Conference, CRC for Clean Power from Lignite*, 113-118 (2000).

Huynh, D., Doguparthy, S., Ellis, H., Underwood, R. and McIntosh, M., "Largest 'Lignite Briquette' ever made using MTE dewatering process," *Proceedings of Eighth Annual Conference*, *CRC for Clean Power from Lignite*, 17-22 (2001).

Hupa, M., Skrifvars, B.-J. and Moilanen, A., "Measuring the sintering tendency of ash by a laboratory method," *J. Inst. Energy*, September, 131-137 (1989).

Jéquier, L., Longchambon, L. and Van de Putte, G., "The gasification of coal fines," *Inst. of Fuel Journal*, 33, 584-591 (1960).

Kemezys, M. and Taylor, G.H., "Occurrence and distribution of minerals in some Australian coals," *J. Inst. Fuel*, 37, 389-397 (1964).

Kikuchi, K., Suzuki, A., Mochizuki, T., Endo, S., Imai, E. and Tanji, Y., "Ash-agglomerating gasification of coal in a spouted bed reactor," *Fuel*, 64, 368-372 (1985).

Kiss, L.T. and King, T.N., "Reporting of low-rank coal analysis – the distinction between minerals and inorganics," *Fuel*, 58, 547-549 (1979).

Kiss, L.T. and King, T.N., "The expression of results of coal analysis: the case for brown coals," *Fuel*, 56, 340-341 (1977).

Kolodney, M., Yerushalmi, J., Squires, A.M. and Harvey, R.D., "The behaviour of mineral matter in a fluidized bed gasifying coal – The Ignifluid process," *Trans. and Journal of the Br. Ceramic Society*, 75, 85-91 (1976).

Kosminski, A., "Reactions between sodium and silicon minerals during gasification of low-rank coal," *The University of Adelaide* (2001), PhD Thesis.

Kosminski, A., “Reactions of sodium with silica and kaolin during gasification of low-rank coal - thermodynamic considerations,” *CRC for Clean Power from Lignite*, Internal Report No. 00003, May (2000a).

Kosminski, A., “Reactions of sodium with silica and kaolin. Laboratory scale gasification. Initial experimental results.” *Proc. of Fourth Annual Conference, CRC New Technologies for Power Generation from Low-rank Coal*, 161-167 (1997).

Kosminski, A., “Reactions of sodium with silica during gasification of coal – laboratory scale investigations,” *Proceedings of Seventh Annual Conference, CRC for Clean Power from Lignite*, 67-72 (2000b).

Kosminski, A., “Transformations of sodium in high-sulphur lignite during pyrolysis and gasification,” *Proc. of Sixth Annual Conference, CRC New Technologies for Power Generation from Low-rank Coal*, 145-152 (1999).

Kosminski, A. and Manzoori, A.R., “Inorganic matter behaviour in the gasification of South Australian coals for combined cycle power generation,” *Technical Services Department*, *Electricity Trust of South Australia*, Technical Report, September (1990).

Kracek, F.C., “Phase equilibrium relations in the system, Na_2SiO_3-Li_2SiO_2-SiO_2,” *J. Am. Chem. Soc.*, 61(10), 2863-2877 (1939).

Kuczynski, G.C., “Self-diffusion in sintering of metallic particles,” *Am. Inst. of Mining and Metallurgy Engineers Transactions*, 185, 169-178 (1949).

Kunii, D. and Levenspiel, O., *Fluidization Engineering*, 2nd edition, Butterworth-Heinemann (1991).

Langston, B.G. and Stephens, F.M. (Jr.), “Self-agglomerating fluidized-bed reduction,” *Journal of Metals*, April, 312-316 (1960).

Lim, K.S., Peeler, P.K., Zakhari, A. and Bhattacharya, S.P., "Design of the CRC's Pressurized PDU for Lignite Gasification and Char Combustion," *Proceedings of Seventh Annual Conference, CRC for Clean Power from Lignite*, 25-30 (2000).

Liss, B., Blake, T.R., Squires, A.M. and Bryson, R., "Incipient defluidization of sinterable solids," *Proc. of Fourth Int. Conf. on Fluidization*, 249-256 (1983).

Loehden, D., Walsh, P.M., Sayre, A.N., Beer, J.M., and Sarofim, A.F., "Generation and deposition of fly ash in the combustion of pulverised coal," *Journal of the Institute of Energy*, 62(451), 119-127 (1989).

Mansaray, K.G. and Ghaly, A.E., "Agglomeration characteristics of alumina sand-rice husk ash mixtures at elevated temperatures," *Energy Sources*, 19, 1005-1025 (1997).

Manzoori, A.R., "Role of the inorganic matter in agglomeration and defluidisation during the circulating fluid bed combustion of low-rank coals," *The University of Adelaide* (1990), PhD Thesis.

Manzoori, A.R. and Agarwal, P.K., "Agglomeration and defluidization under simulated fluidized-bed combustion conditions," *Fuel*, 73, 563-568 (1994).

Manzoori, A.R. and Agarwal, P.K., "The fate of organically bound inorganic elements and sodium chloride during fluidized bed combustion of high sodium, high sulphur low rank coals," *Fuel*, 71, 513-522 (1992).

Marinov, V., Marinov, S.P., Lazarov, L. and Stefanova, M., "Ash agglomeration during fluidized bed gasification of high sulphur content lignites," *Fuel Processing Technology*, 31, 181-191 (1992).

Mason, D.M., "The behavior of iron-sulfur species in fluidized-bed gasification on coal," *Fuel Processing Technology*, 30, 215-226 (1992).

Mason, D.M. and Patel, J.G., "Chemistry of ash agglomeration in the U-GAS process," *Fuel Processing Technology*, 3, 181-206 (1980).

Mathur, K.B. and Gishler, P.E., "A technique for contacting gases with coarse solid particles," in Altwicker and Konduri (1992), p177.

Matsen, J.M., "Scale-up of fluidized bed processes: principle and practice," *Powder Technology*, 88, 237-244 (1996).

McIntosh, M., "Repowering – Is this practicable for improving the efficiency of lignite fuelled boiler plant?" *Proceedings of Seventh Annual Conference, CRC for Clean Power from Lignite*, 7-12 (2000).

McLaughlin, L.J., "Defluidisation: A study of the influence of liquid and their properties on gas fluidised behaviour," *PhD Thesis*, *Monash University* (1999).

Mikami, T., Kamiya, H. and Horio, M., "The mechanism of defluidization of iron particles in a fluidized bed," *Powder Technology*, 89, 231-238 (1996).

Mody, D. and Li, C.-Z., "Transformation of alkali and alkaline earth metals during the pyrolysis of a lignite," *Proceedings of Seventh Annual Conference, CRC for Clean Power from Lignite*, 49-54 (2000).

Mody, D., Wu, H. and Li, C.-Z., "Fates and roles of alkali and alkaline earth metal species during the pyrolysis and gasification of a Victorian lignite," *Proceedings of the Ninth Australian Coal Science Conference*, Brisbane, QLD, 26^{th}-29^{th} November (2000), published on CD-ROM.

Mojtahedi, W. and Backman, R., "Release of alkali metals in pressurised fluidised-bed combustion and gasification of peat," *Technical Research Centre of Finland*, Report No. 53, March (1989a), p48.

Mojtahedi, W. and Backman, R., "The fate of sodium and potassium in the pressurised fluidised-bed combustion and gasification of peat," *J. Inst. Energy*, December, 189-196 (1989b).

Mojtahedi, W., Kurkela, E. and Nieminen, M., "Release of sodium and potassium in the PFB gasification of peat," *J. Inst. Energy*, September, 95-100 (1990).

Morey, G.W. and Bowen, N.L., "The binary system sodium metasilicate-silica," *J. Phys. Chem.*, 28(11), 1167-1179 (1924).

Morey, G.W. and Ingerson, E., "The system, water-sodium disilicate," *American Journal of Science*, 5th Series, 35-A, 217-225 (1938).

Murray, J.B., "Changes in state of combination of inorganic constituents during carbonization of Victorian brown coal," *Fuel*, 52, 105-111 (1973).

Natarajan, E., Ohman, M., Gabra, M., Nordin, A., Liliedah, T., and Rao, A.N., "Experimental determination of bed agglomeration tendencies of some common agricultural residues in fluidized bed combustion and gasification," *Biomass and Bioenergy*, 15(2), 163-169 (1998).

Peters, W., "Fundamentals of coal gasification," (1976); cited in Ward (1984), p134.

Poeze, A. and Zhang, D.-K., "Variation of sodium forms and char reactivity during gasification of a South Australian low-rank coal," *Proceedings of Seventh Annual Conference, CRC for Clean Power from Lignite*, 61-66 (2000).

Qi, Y. and Chaffee, A.L., "Characterisation of organic and inorganic components in product water from novel coal drying process – background and methodology," *Proceedings of Seventh Annual Conference, CRC for Clean Power from Lignite*, 143-148 (2000).

Qi, Y. and Chaffee, A.L., "Effects of processing conditions on the nature of product water from a novel coal drying process," *Proceedings of Eighth Annual Conference*, *CRC for Clean Power from Lignite*, 41-46 (2001).

Rawson, H., "Properties and applications of glass," *Glass Science and Technology Vol. 3*, Elsevier, (1980).

Readett, D.J. and Quast, K.B., "Minerals and inorganics associated with South Australian lignites – final report," *S.A. Institute of Technology*, Report to S.E.N.R.A.C., December (1987).

Rehmat, A. and Saxena, S.C., "Agglomeration of ash in fluidized-bed gasification of coal by steam-oxygen (or air) mixture," *Ind. Eng. Chem. Process Des. Dev.*, 19, 223-230 (1980).

Rosin, P. and Rammler, E., "The laws governing the fineness of powdered coal," *The Institute of Fuel*, 7(31), 29-36 (1933).

Schad, M.K. and Hafke, C.F., "Recent developments in coal gasification," *Chemical Engineering Progress*, 79(5), 45-51 (1983).

Schafer, H.N.S., "Chapter 7: Functional groups and ion exchange properties," in *The Science of Victorian Brown Coals: Structure, Properties and Consequences for Utilization*, edited by Durie, R.A., Butterworth-Heinemann (1991), 323-357.

Schafer, H.N.S., "Organically bound iron in brown coals," *Fuel*, 56, 45-46 (1977).

Schafer, H.N.S., "Pyrolysis of brown coals. 1. Decomposition of acid groups in coals containing carboxyl groups in the acid and cation forms," *Fuel*, 58, 667-672 (1979a).

Schafer, H.N.S., "Pyrolysis of brown coals. 2. Decomposition of acidic groups on heating in the range 100-900°C," *Fuel*, 58, 673-679 (1979b).

Seville, J.P.K., Silomon-Pflug, H. and Knight, P.C., "Modelling of sintering in high temperature gas fluidisation," *Powder Technology*, 97, 160-169 (1998).

Seville, J.P.K., Willett, C.D. and Knight, P.C., "Interparticle forces in fluidisation: a review," *Powder Technology*, 113, 261-268 (2000).

Siegell, J. H., "High-temperature defluidization," *Powder Technology*, 38, 13-22 (1984).

Smith, E.J.D., "The sintering of fly-ash," *J. Inst. Fuel*, June, 253-260 (1956).

Stallmann, J.J. and Neavel, R.C., "Technique to measure the temperature of agglomeration of coal ash," *Fuel*, 59, 584-586 (1980).

Sue-A-Quan, T.A., Cheng, G. and Watkinson, A.P., "Coal gasification in a pressurized spouted bed," *Fuel*, 74(2), 159-164 (1995).

Thiessen, G., "Chapter 14: Composition and origin of the mineral matter in coal," *Chemistry of Coal Utilization*, *Volume 1*, edited by Lowry, H.H., John Wiley & Sons (1945), 485-495.

Tomita, A. and Ohtsuka, Y., "Chapter 5: Gasification and combustion of brown coal," *Advances in the Science of Victorian Brown Coal*, edited by Li, C.-Z., Elsevier (2004), 223-285.

Trewin, D., "Energy and Greenhouse Gas emissions accounts, Australia: 1992-93 to 1997-98," *Australian Bureau of Statistics (ABS)*, ABS Catalogue No. 4604.0 (2001), pp20, 55, 57.

Tsai, S.C., *Fundamentals of Coal Beneficiation and Utilization*, Coal Science and Technology Series, 2, Elsevier Scientific Publishing Company (1982).

U.S. Department of Energy, *Coal Gasification: Technology Status Report*, Morgantown Energy Technology Center, U.S. Department of Energy, August (1986).

Varshneya, A.K., *Fundamentals of Inorganic Glasses*, Academic Press (1993), p570.

Vassilev, S.V., Eskenazy, G.M. and Vassileva, C.G., "Contents, modes of occurrence and behaviour of chlorine and bromine in combustion wastes from coal-fired power stations," *Fuel*, 79, 923-937 (2000).

Vuthaluru, H.B., "Behaviour of inorganic constituents during fluidised-bed combustion of low-rank coals - effect of temperature on ash characteristics," *CRC for Clean Power from Lignite*, Internal Report No. 99019, (1999a).

Vuthaluru, H.B., "Mitigation of ash problems in fluidised-bed combustion systems using alternative bed materials," *CRC for Clean Power from Lignite*, Internal Report No. 99027, (1999b).

Vuthaluru, H.B., "Remediation of ash problems in fluidised bed combustion," *CRC for Clean Power from Lignite*, Internal Report No. 99029, (1999c).

Vuthaluru, H.B., "Role of calcium and magnesium during fluidised bed combustion of a South Australian low-rank coal," *CRC for Clean Power from Lignite*, Internal Report No. 99028, (1999d).

Vuthaluru, H.B., Eenkhoorn, S., Hamburg, G., Heere, P.G.T. and Kiel, J.H.A., "Behaviour of iron-bearing minerals in the early stages of pulverised coal conversion processes," *Fuel Processing Technology*, 56, 21-31 (1998).

Wall, C.J., Graves, J.T. and Roberts, E.J., "How to burn salty sludges," *Chemical Engineering*, 82, 77-82 (1975).

Ward, C.R. (editor), *Coal Geology and Coal Technology*, Blackwell Scientific Publications (1984), 134-138.

Warne, S.St.J., "Coal mineral reactions," *Coal: Properties, Analysis and Effective Use*, edited by Wall, T.F., The Institute of Coal Research, University of Newcastle (1982a), 8p.

Warne, S.St.J., "Introduction to minerals in coal," *Coal: Properties, Analysis and Effective Use*, edited by Wall, T.F., The Institute of Coal Research, University of Newcastle (1982b), 11p.

Watkinson, A.P., Cheng, G. and Prakash, C.B., "Comparison of coal gasification in fluidized and spouted beds," *The Canadian Journal of Chemical Engineering*, 61, 468-477 (1983).

Wibberley, L.J., "Furnace deposits and corrosion," *Coal: Properties, Analysis and Effective Use*, edited by Wall, T.F., The Institute of Coal Research, University of Newcastle (1982), 22p.

Wiggering, *Chem. Geol.*, 85, 311 (1990).

Yang, W.-C. and Keairns, D.L., "Operational analysis of ash-agglomerating fluidized bed gasifiers," *Powder Technology*, 111, 168-174 (2000).

Yerushalmi, J., Kolodney, M., Graff, R.A., Squires, A.M. and Harvey, R.D., "Agglomeration of ash in fluidized beds gasifying coal: The Godel phenomenon," *Science*, 187, 646-648 (1975).

APPENDICES

APPENDIX A

CALCULATION PROCEDURES

A.1 Introduction

In this Appendix, the calculation procedures for determining experimental operating parameter values, inlet gas velocity of the steam-air mixture to the bed, and terminal velocity of 3.35 mm diameter particles are detailed. Sample calculations are provided in each case.

A.2 Experimental Operating Parameters

Values for operating parameters and settings for each experiment were calculated as follows:

1. Desired steam concentration of the fluidising gas is set, in the form of steam-to-air mass ratio;
2. Desired air-to-fuel mass ratio (A/F), or steam-to-fuel mass ratio (S/F), is set;
3. Desired superficial velocity (U_s), based on cylindrical diameter of gasifier, is set;
4. Externally-controlled furnace temperature (T_f) is set;
5. Maximum bed temperature (T_{max}) is assumed, based on a value approximately 100°C greater than the T_f set-point value;
6. Total volumetric flow rate is calculated using Equation A.1:

$$Q_{gas} = U_s \times \pi/4 \times (D_{cylindrical})^2 \qquad \text{(A.1)}$$

7. The composition of the steam-air gas mixture is calculated using the following steps:
    a. The gas component mass fractions (m_i, where i = O_2, N_2 or H_2O) are calculated by adding S/A ratio to the typical air composition of 23.3 wt% O_2 and 76.7 wt% N_2, and normalising against a total of 1.0.

b. The gas component mole fractions (n_i, where i = O_2, N_2 or H_2O) are calculated by multiplying m_i by the molecular weight of the component (MW_i), as in Equation A.2, and normalising against a total of 1.0.

$$n_i = m_i \times MW_i \qquad (A.2)$$

c. Calculate the total molecular weight of the steam-air gas mixture (MW_{gas}) by multiplying the mole fraction of each gas component by its molecular weight, and summing together, as in Equation A.3.

$$MW_{gas} = \sum[n_i \times MW_i], \quad i = O_2, N_2, H_2O \qquad (A.3)$$

8. Calculate the volumetric flow rate of each gas component (Q_i) by multiplying Q_{gas} by the mole fraction of each component, as shown in Equation A.4.

$$Q_i = Q_{gas} \times n_i, \quad i = O_2, N_2, H_2O \qquad (A.4)$$

9. Volumetric flow rate of air at STP conditions ($Q_{air(STP)}$), is calculated via Equation A.5. This forms the set-point value used for the variable-area flow meter.

$$Q_{air(STP)} = (Q_{O2} + Q_{N2}) \times (298\ K / T_{max}) \qquad (A.5)$$

10. Calculate mass flow rates of coal and steam using the following calculation method:

a. Calculate the density of the gas at process conditions, using process pressure (P), MW_{gas}, gas constant (R), and T_{max}, as in Equation A.6.

$$\rho_{gas} = (P \times MW_{gas}) / (R \times T_{max}) \qquad (A.6)$$

b. Calculate the total mass flow rate of the steam-air mixture using Equation A.7.

$$M_{gas} = Q_{gas} \times \rho_{gas} \qquad (A.7)$$

c. Calculate the mass flow rate of each individual component (M_i) by multiplying the mass fraction of each component by M_{gas}, as in Equation A.8.

$$M_i = m_i \times M_{gas}, \quad i = O_2, N_2, H_2O \tag{A.8}$$

d. Calculate the coal feed rate (dry basis) by dividing air mass rate (i.e. M_{O2} + M_{N2}) by A/F, as shown in Equation A.9.

$$M_{coal} = (M_{O2} + M_{N2}) / (A/F) \tag{A.9}$$

11. At the completion of the experiment, the actual recorded maximum bed temperature ($T_{max,rec}$) is used to recalculate U_s. This is necessary given that the calculated process gas flow rate varies with bed temperature, which in turn changes the calculated mass flow rates of the gas components, and hence A/F and S/F. In reality, only volumetric flow rate varies with temperature, while mass flow rate remains constant. Desired superficial velocity, U_s, is altered using trial and error, until A/F and S/F match the original desired value.

The following shows the sample calculations that were performed for Run A02.

- Set the desired operating parameters as in Steps 1-4 above, including:
  - S/A ratio = 0.13
  - A/F ratio = 3.0
  - U_s = 0.60 m/s
  - T_f = 825°C

- Bed temperature is assumed following Step 5:
  - T_{max} = 925°C

- Calculate the total volumetric flow rate of the steam-air mixture through the bed using Equation A.1:

$$Q_{gas} = U_s \times A_{x\text{-section}}$$

$= (0.60 \text{ m/s}) \times \pi/4 \times (0.076 \text{ m})^2$

$= 0.0027 \text{ m}^3/\text{s}$

- Calculate the steam-air mixture gas composition following Steps 7a to 7c. Refer to Table A.1 for tabulated results of calculations.

Table A.1. Calculated mass and mole fractions of components in steam-air mixture for Run A02.

Component	Molecular weight (kg/kmol)	Mass, based on 1 kg air (kg)	Mass fraction	Moles, based on 1 kg air (kmol)	Mole fraction	Weighted molecular weight (kg/kmol)
H_2O	18	0.13	0.12	0.0064	0.17	3.1
O_2	32	0.23	0.21	0.0064	0.17	5.6
N_2	28	0.77	0.68	0.024	0.65	18.3
Total	-	1.13	1.00	0.037	1.00	27.0

- Calculate the volumetric flow rate of each gas component as in Step 8. Refer to Table A.2 for results of calculations.

Table A.2. Volumetric and mass flow rates of gas components in steam-air gas mixture.

Component	Volumetric flow rate (m^3/s)	Volumetric flow rate (LPM)	Mass flow rate (kg/s)	Mass flow rate (kg/h)
H_2O	0.47×10^{-3}	28.1	0.86×10^{-4}	0.31
O_2	0.47×10^{-3}	28.4	1.5×10^{-4}	0.55
N_2	1.78×10^{-3}	106.7	5.1×10^{-4}	1.82
Total	2.72×10^{-3}	163.2	7.4×10^{-4}	2.68

- Determine the STP air flow rate following Step 9 above:

$Q_{air(STP)} = (Q_{O2} + Q_{N2}) \times (298 \text{ K} / T_{max})$

$= (28.4 + 106.7) \times (298/[925+273])$

$= 33.6 \text{ LPM}$

- Calculate the density of the gas at process conditions using Equation A.6:

$\rho_{gas} = (P \times MW) / (R \times T_{max})$

$= (101 \text{ kPa} \times 27.0 \text{ kg/kmol}) / (8.314 \text{ kPa.m}^3/\text{kmol.K} \times 1198 \text{ K})$

$= 0.273\ kg/m^3$

- Calculate the total mass flow rate of the steam-air mixture using Equation A.7:

$$M_{gas} = Q_{gas} \times \rho_{gas}$$
$$= 0.0027 \times 0.273$$
$$= 7.4\times10^{-4}\ kg/s$$

- Calculate the mass flow rate of each individual component using Equation A.8 (results shown in Table A.2). This indicates a mass flow rate of steam of 0.31 kg/h, or a feed water flow rate of approximately 5.1 g/min.

- Calculate the coal feed rate (dry basis) using Equation A.9:

$$M_{coal} = (M_{O2} + M_{N2}) / (A/F)$$
$$= (0.55 + 1.82) / 3.0$$
$$= 0.77\ kg/hr$$

- At the completion of the experiment, the maximum bed temperature was measured at 920°C. Trial-and-error altering of U_s resulted in an actual superficial velocity of 0.59 m/s achieved in the bed.

A.3 Inlet Gas Velocity

The gas velocity at the inlet to the bed (i.e. at the conical gas distributor level) differs from the superficial velocity, U_s, due to a lower gas temperature at the inlet, and a smaller orifice through which the gas passes. The inlet velocity, U_{inlet}, is calculated using the following calculation method:

1. Gas density at the inlet ($\rho_{gas,\ inlet}$) is calculated using Equation A.6, but with substitution of T_{max} with the temperature recorded at TC1 (T_{inlet}), as in Equation A.10.

$$\rho_{gas,\ inlet} = (P \times MW_{gas}) / (R \times T_1) \quad (A.10)$$

2. Flow rate of the gas at the inlet ($Q_{gas,\ inlet}$) is calculated by dividing mass flow rate of the gas (M_{gas}), as calculated in Equation A.7, by $\rho_{gas,\ inlet}$. This is shown in Equation A.11.

$$Q_{gas,\ inlet} = M_{gas} / \rho_{gas,\ inlet} \quad (A.11)$$

3. U_{inlet} is calculated by dividing $Q_{gas,\ inlet}$ by the cross-sectional area of the inlet orifice, as in Equation A.12.

$$U_{inlet} = Q_{gas,\ inlet} / (\pi/4 \times D_{inlet}^2) \quad (A.12)$$

The following shows the sample calculations that were performed for Run A02.

- Gas density is calculated using Equation A.10.

$$\rho_{gas,\ inlet} = (P \times MW_{gas}) / (R \times T_1)$$
$$= (101\ kPa \times 27.0\ kg/kmol) / (8.314\ kPa.m^3/kmol.K \times 668\ K)$$
$$= 0.49\ kg/m^3$$

- Inlet gas flow rate is calculated using Equation A.11.

$$Q_{gas,\ inlet} = M_{gas} / \rho_{gas,\ inlet}$$
$$= 7.4\times10^{-4}\ kg/s / 0.49\ kg/m^3$$
$$= 1.5\times10^{-3}\ m^3/s$$

- Inlet gas velocity is calculated using Equation A.12.

$$U_{inlet} = Q_{gas,\ inlet} / (\pi/4 \times D_{inlet}^2)$$
$$= 1.5\times10^{-3}\ m^3/s / (\pi/4 \times 0.012^2)$$
$$= 13.2\ m/s$$

A.4 Terminal Velocity

Terminal velocity calculations were performed in order to determine whether defluidisation (where applicable) was due to ash-related interactions, or if it occurred as a result of insufficient fluidising velocity at the gas inlet to the bed. Terminal velocity (U_t) of the largest particle size to enter the bed, namely 3.35 mm diameter, was calculated in each case. This was compared against the actual gas velocity at the inlet (U_{inlet}), with the particles fluidising when $U_{inlet} > U_t$.

Terminal velocity is calculated via a force balance between drag (F_{drag}), buoyancy ($F_{buoyancy}$) and weight (F_{weight}), using Equations A.13 to A.16. Terminal velocity is contained in the F_{drag} term.

$$F_{total} = F_{drag} - F_{weight} + F_{buoyancy} = 0 \quad (A.13)$$

$$F_{drag} = C_D/2 \times \rho_{gas,\ inlet} \times \pi/4 \times D_p^2 \times U_t^2 \quad (A.14)$$

$$F_{weight} = g \times \pi/6 \times D_p^3 \times \rho_p \quad (A.15)$$

$$F_{buoyancy} = g \times \pi/6 \times D_p^3 \times \rho_{gas,\ inlet} \quad (A.16)$$

Substituting Equations A.14 to A.16 into Equation A.13 and rearranging allows U_t to be calculated, as in Equation A.17.

$$U_t = \sqrt{[(g \times \pi/6 \times D_p^3) \times (\rho_p - \rho_{gas,\ inlet})/(C_D/2 \times \rho_{gas,\ inlet} \times \pi/4 \times D_p^2)]} \quad (A.17)$$

A number of assumptions are made for the calculations, which include:

- Spherical char particle, $D_p = 3.35$ mm;
- Turbulent flow, with Re = 1000, giving $C_D = 1$;
- Particle density, $\rho_p = 1000$ kg/m^3.

Using Run A02 for the sample calculation:

$$U_t = \sqrt{[(g \times \pi/6 \times D_p^3) \times (\rho_p - \rho_{gas,\ inlet})/(C_D/2 \times \rho_{gas,\ inlet} \times \pi/4 \times D_p^2)]}$$

$$= \sqrt{[(9.81 \times \pi/6 \times 0.00335^3) \times (1000 - 0.49)/(1/2 \times 0.49 \times \pi/4 \times 0.00335^2)]}$$

$$= 9.45 \text{ m/s}$$

As U_{inlet} is 13.2 m/s for Run A02, this implies that the largest char particle in the bed is able to fluidise effectively, indicating that defluidisation is a result of particle growth and other ash related reactions.

APPENDIX B

TEMPERATURE AND PRESSURE DROP PROFILES

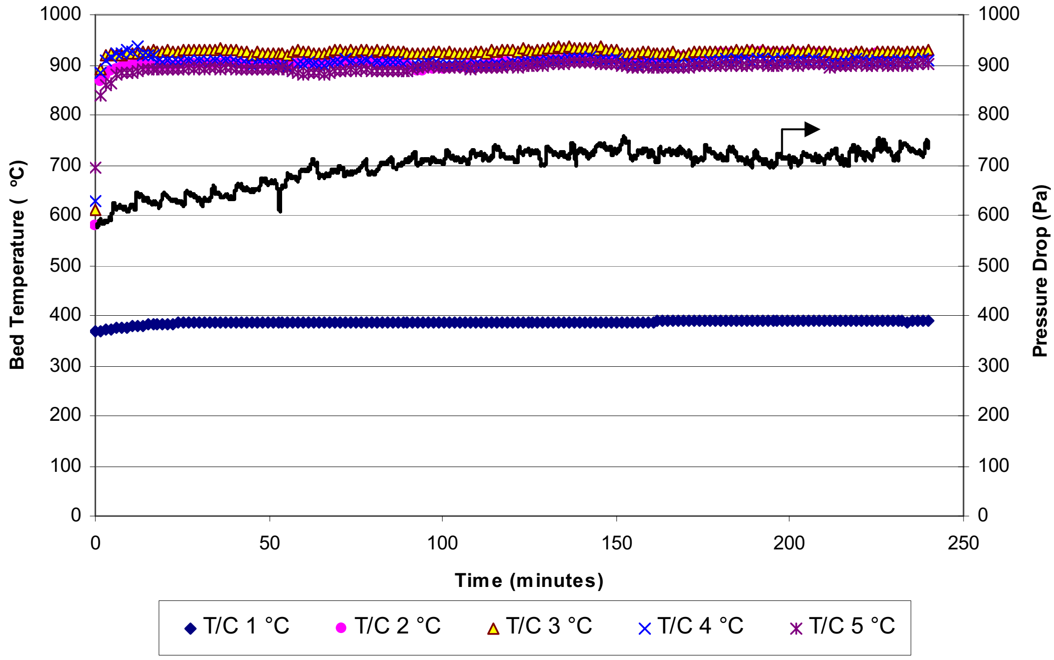

Figure B.1. Temperature and pressure drop profiles for Run A01.

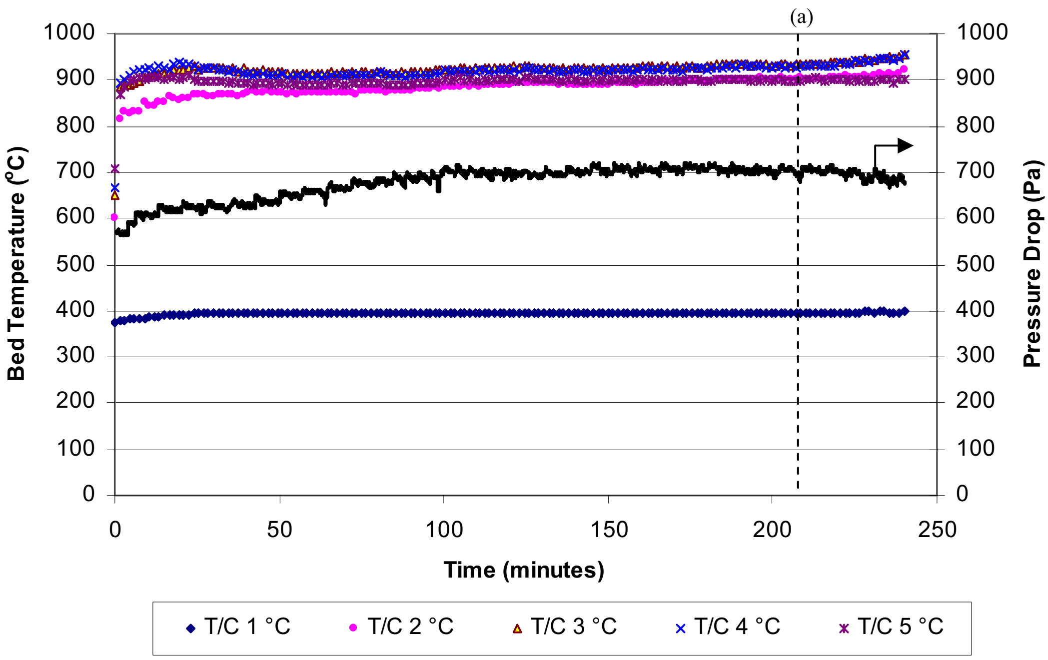

Figure B.2. Temperature and pressure drop profiles for Run A02. Apparent onset of defluidisation indicated by dashed line (a).

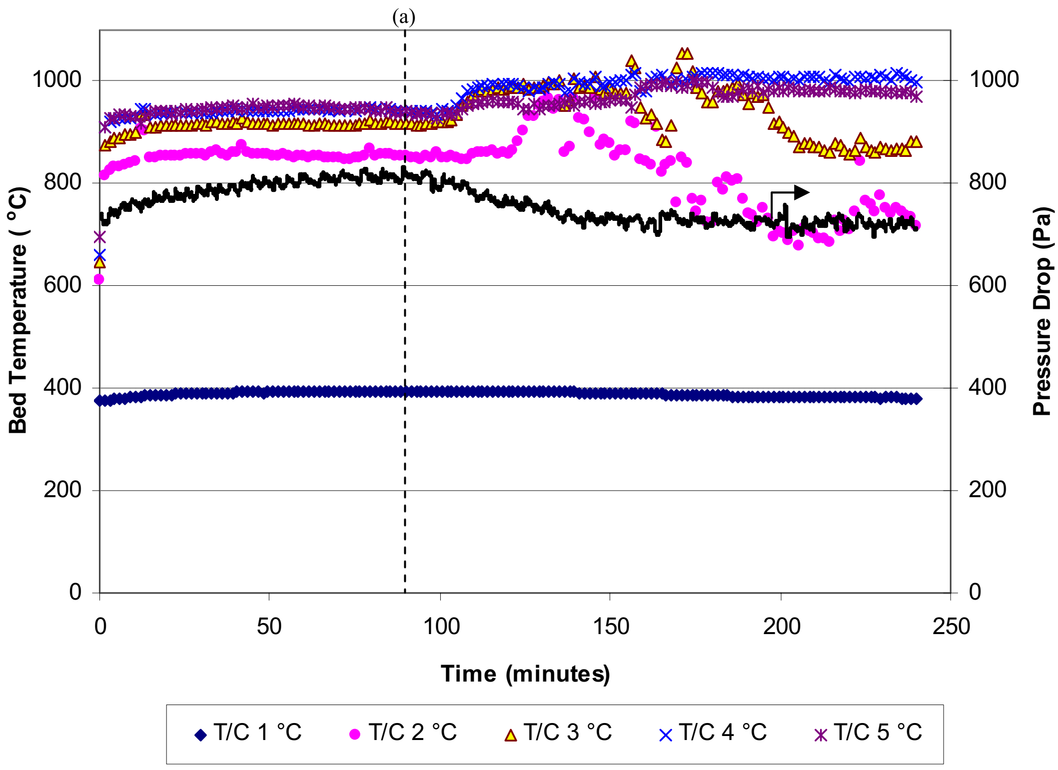

Figure B.3. Temperature and pressure drop profiles for Run A03. Apparent onset of defluidisation indicated by dashed line (a).

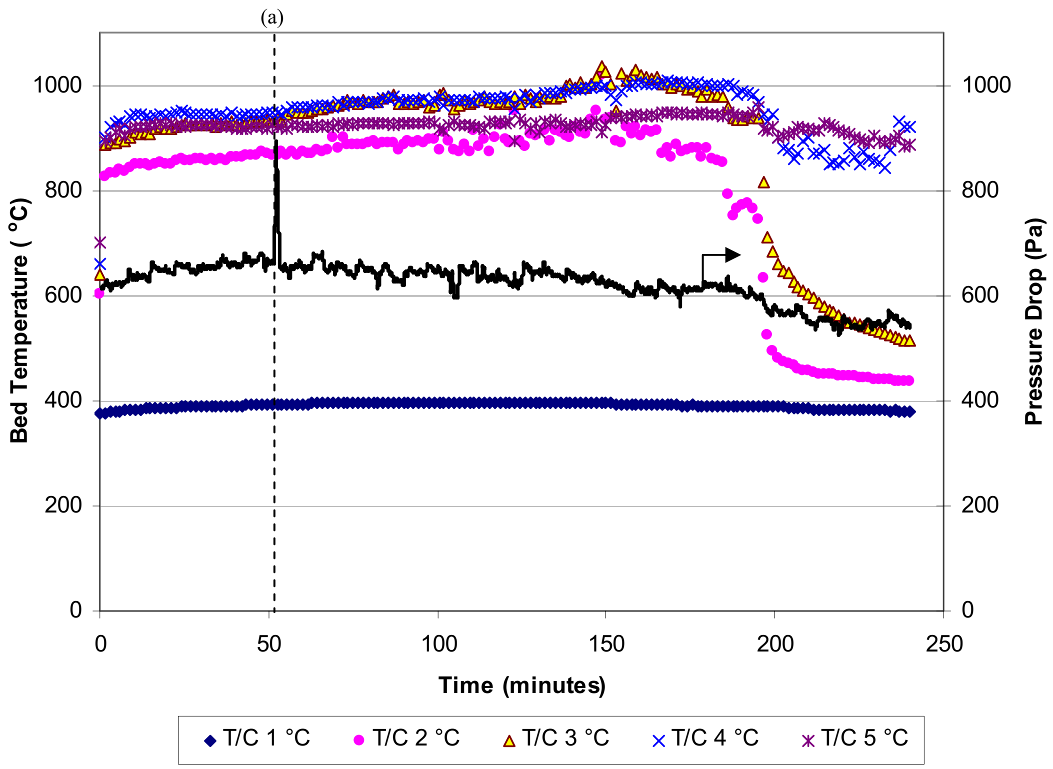

Figure B.4. Temperature and pressure drop profiles for Run A04. Apparent onset of defluidisation indicated by dashed line (a).

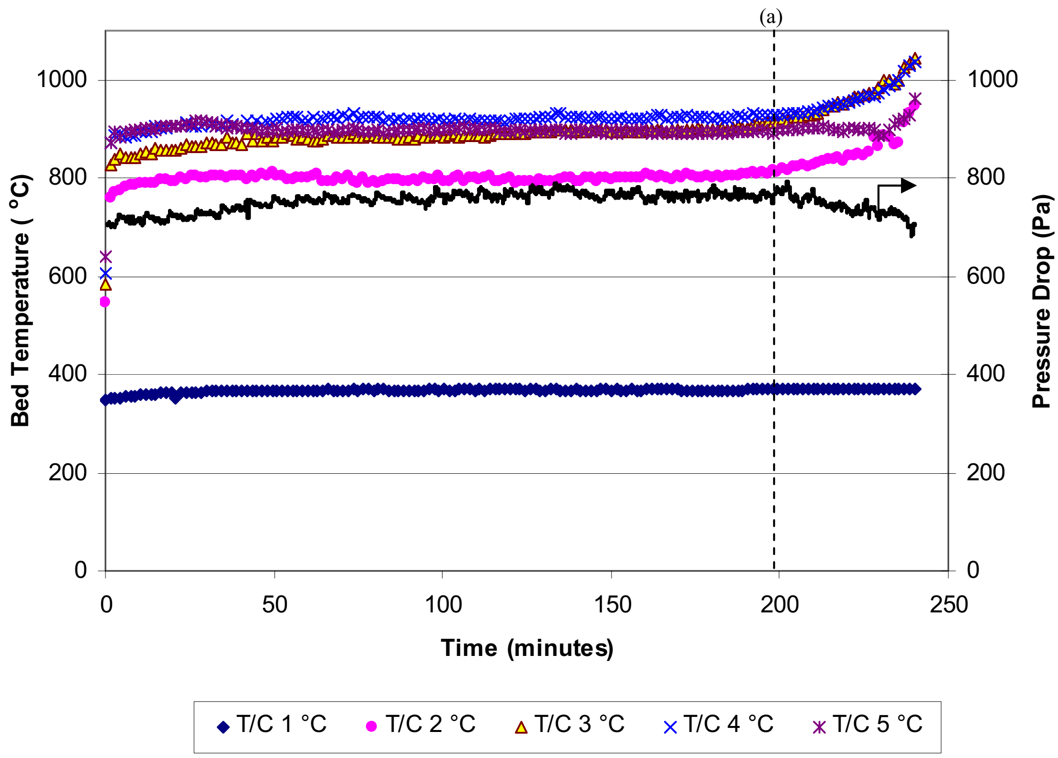

Figure B.5. Temperature and pressure drop profiles for Run A05. Apparent onset of defluidisation indicated by dashed line (a).

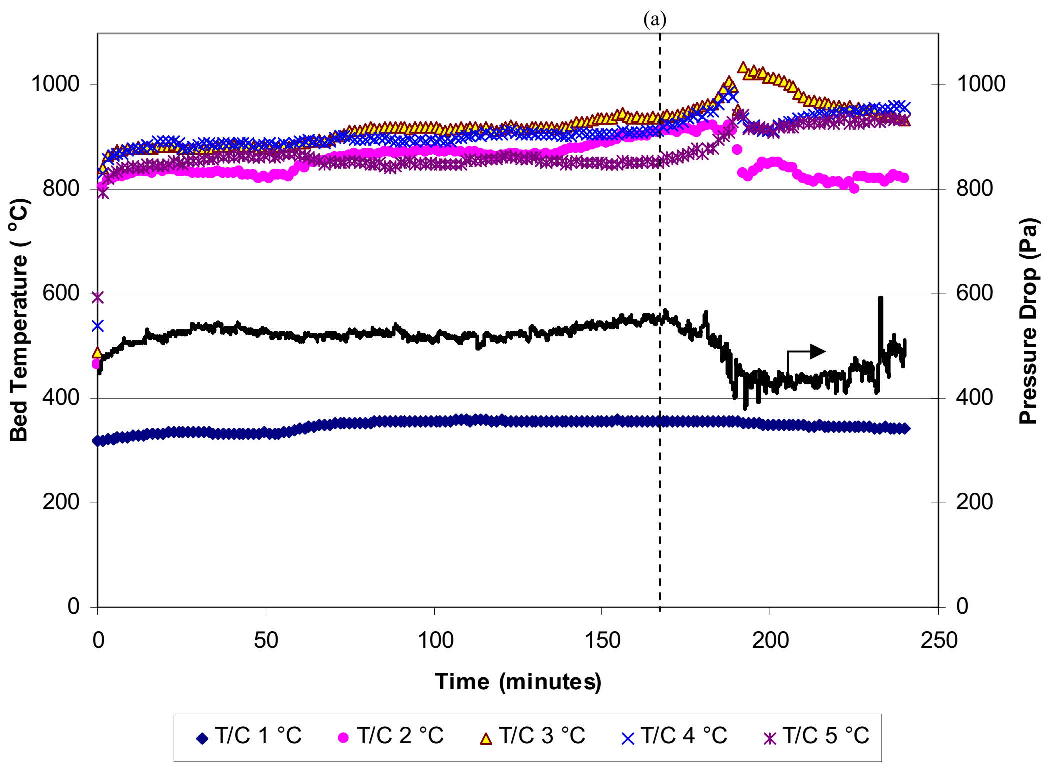

Figure B.6. Temperature and pressure drop profiles for Run A06. Apparent onset of defluidisation indicated by dashed line (a).

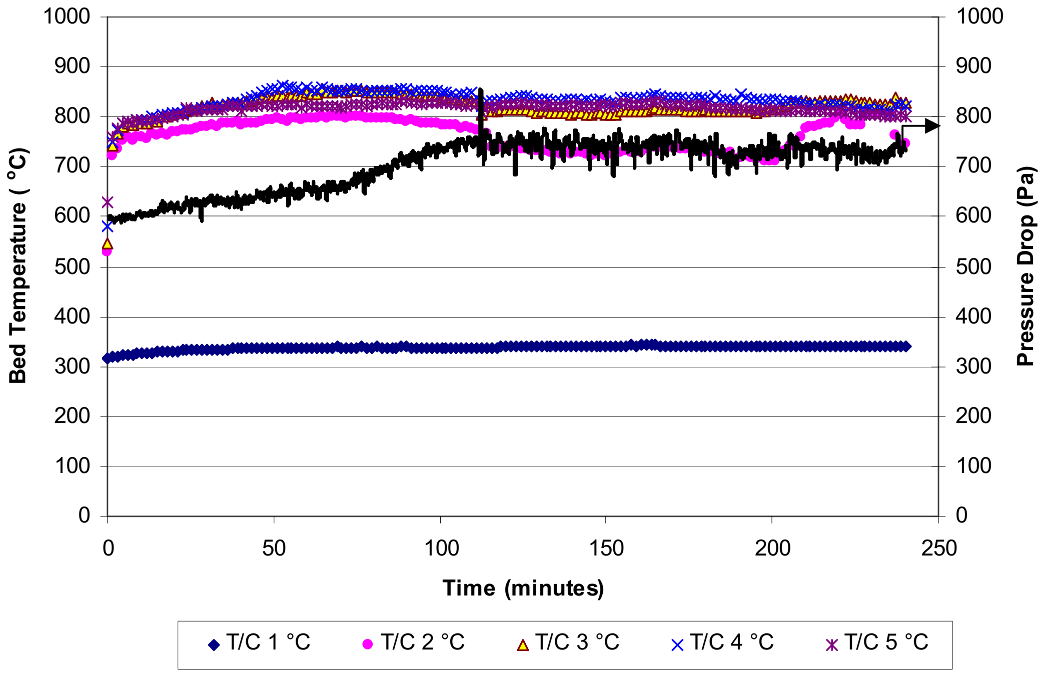

Figure B.7. Temperature and pressure drop profiles for Run B01.

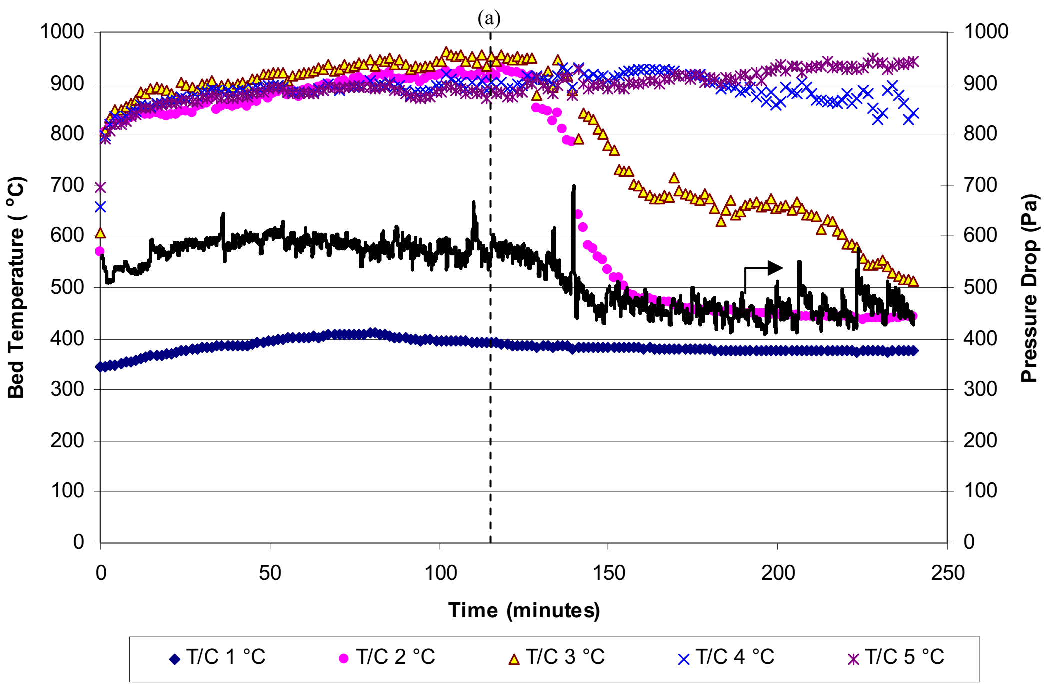

Figure B.8. Temperature and pressure drop profiles for Run B02. Apparent onset of defluidisation indicated by dashed line (a).

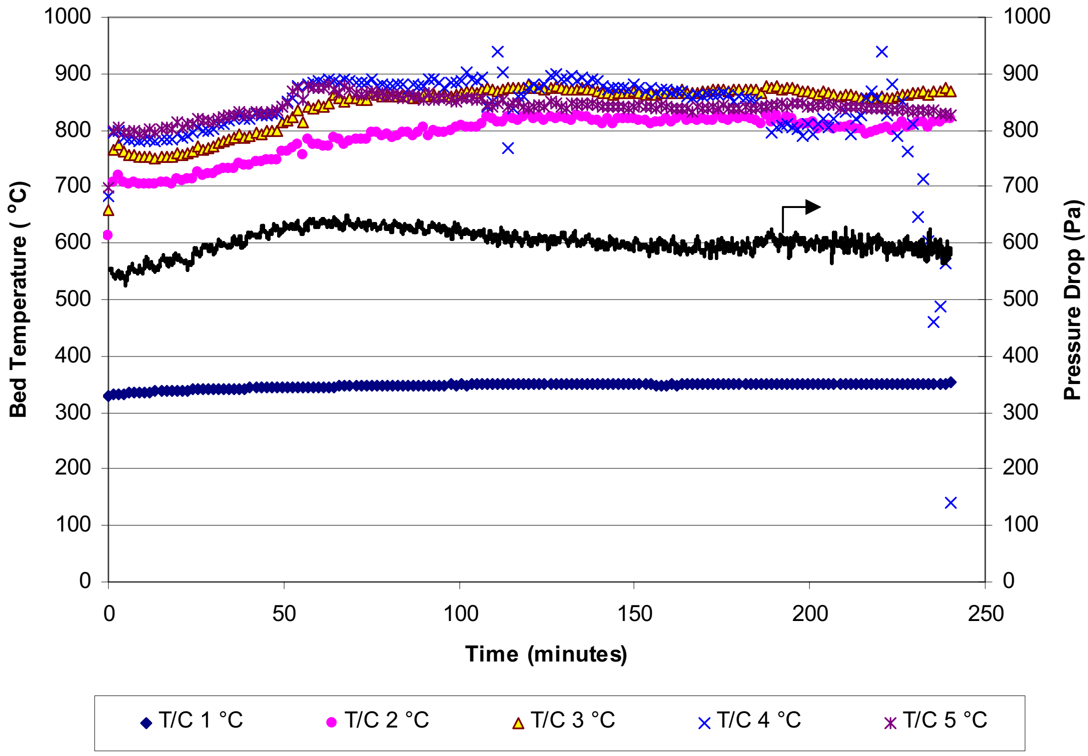

Figure B.9. Temperature and pressure drop profiles for Run B03.

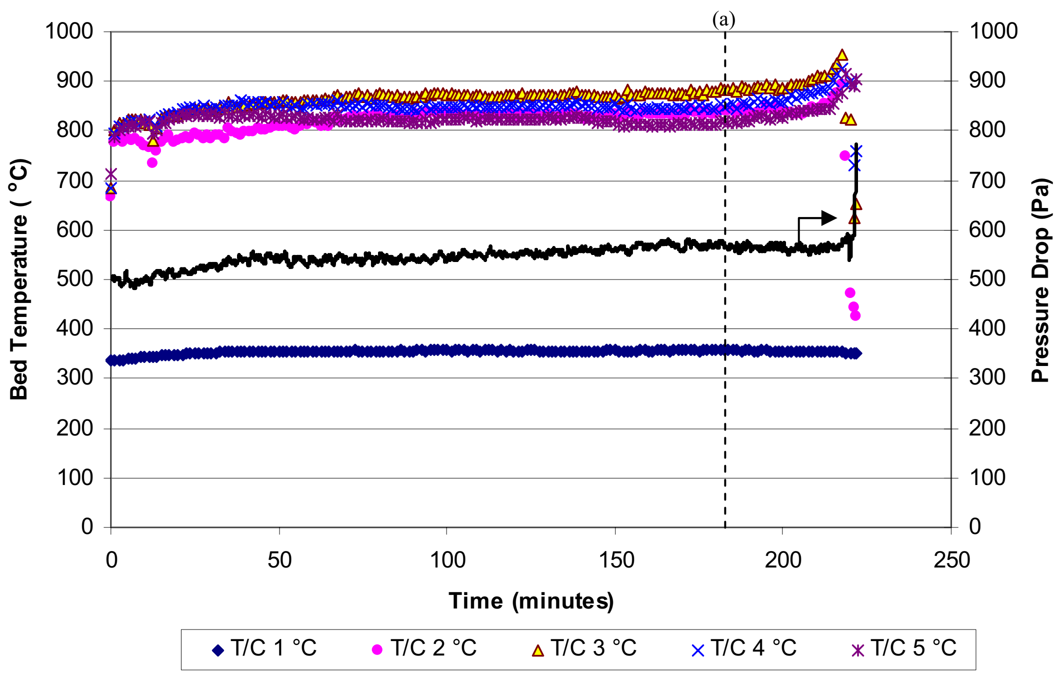

Figure B.10. Temperature and pressure drop profiles for Run B05. Apparent onset of defluidisation indicated by dashed line (a).

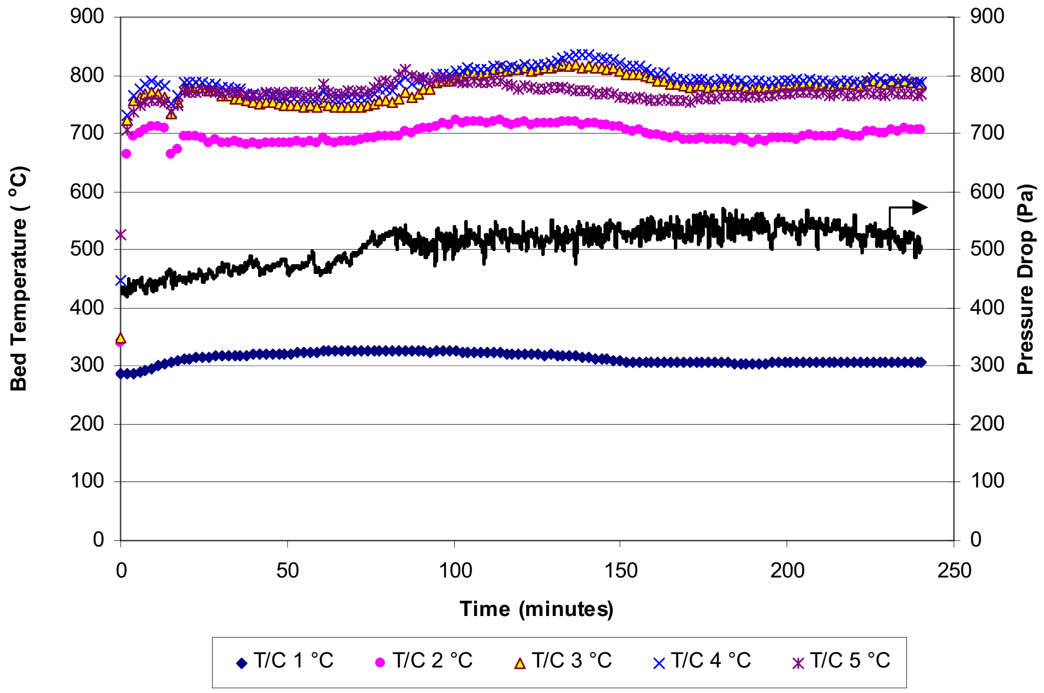

Figure B.11. Temperature and pressure drop profiles for Run B06.

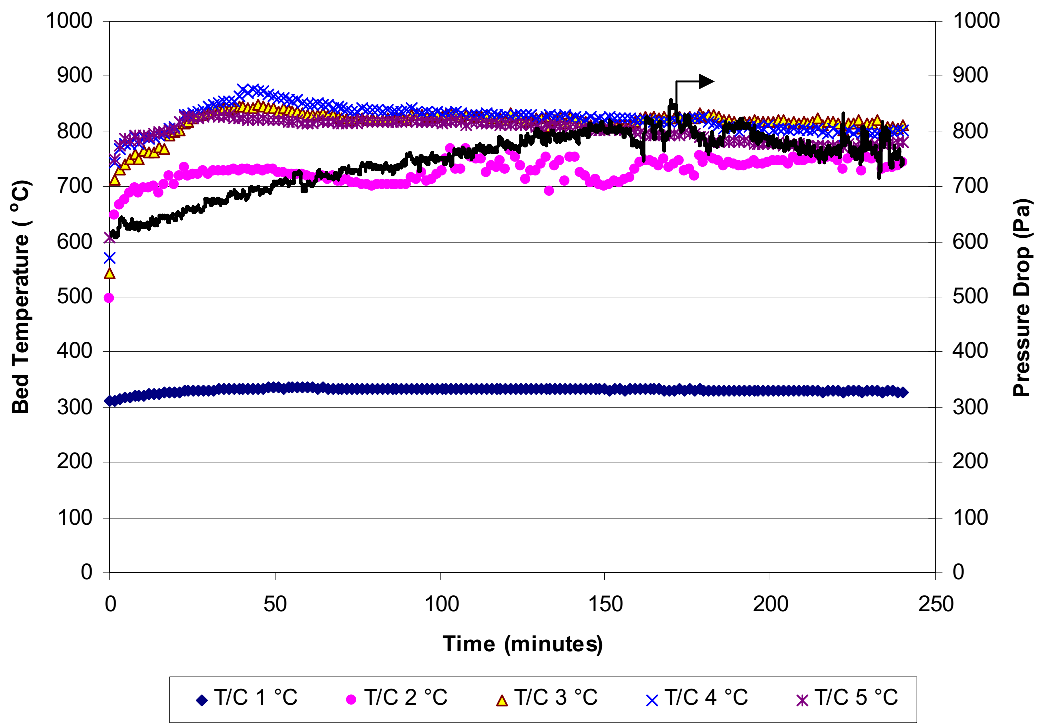

Figure B.12. Temperature and pressure drop profiles for Run B07.

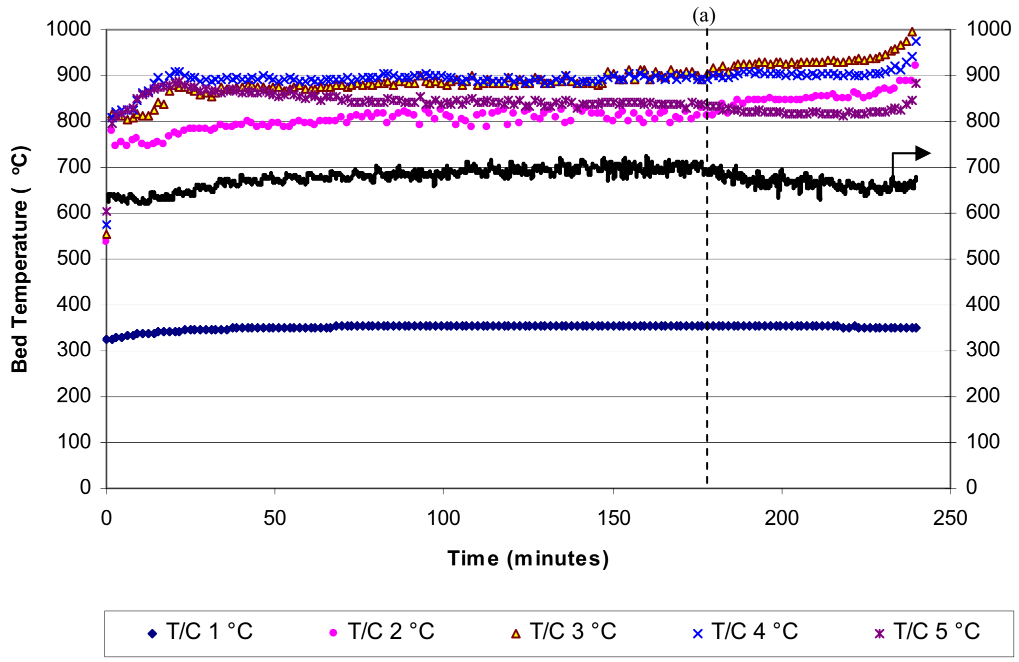

Figure B.13. Temperature and pressure drop profiles for Run B08. Apparent onset of defluidisation indicated by dashed line (a).

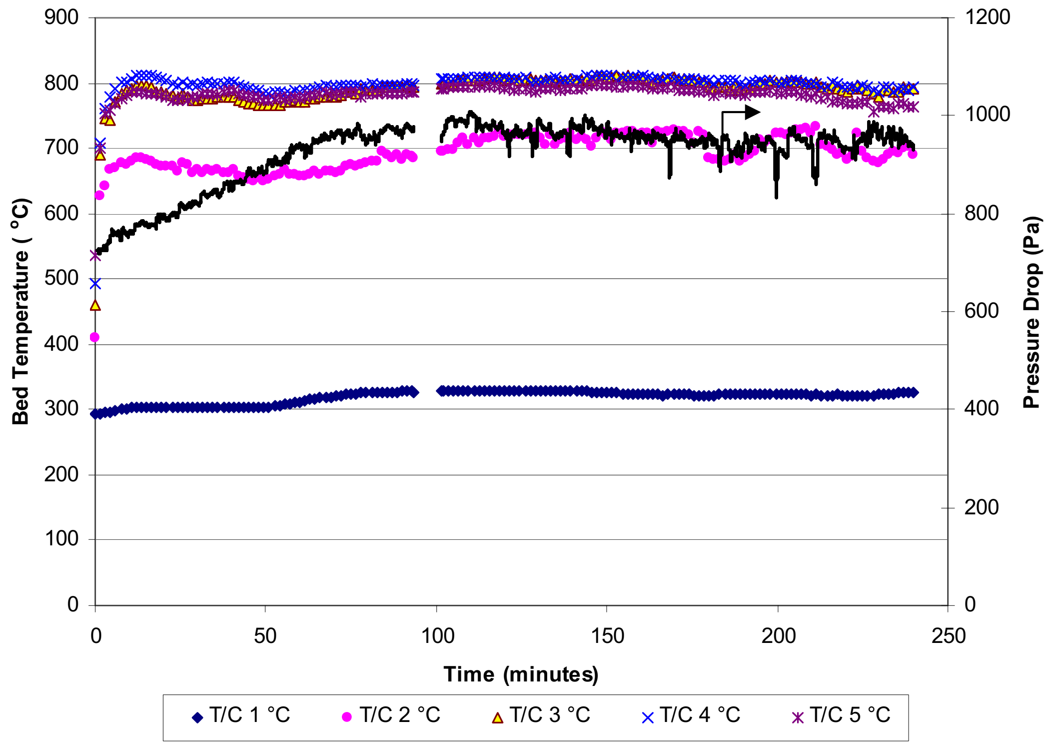

Figure B.14. Temperature and pressure drop profiles for Run B09.

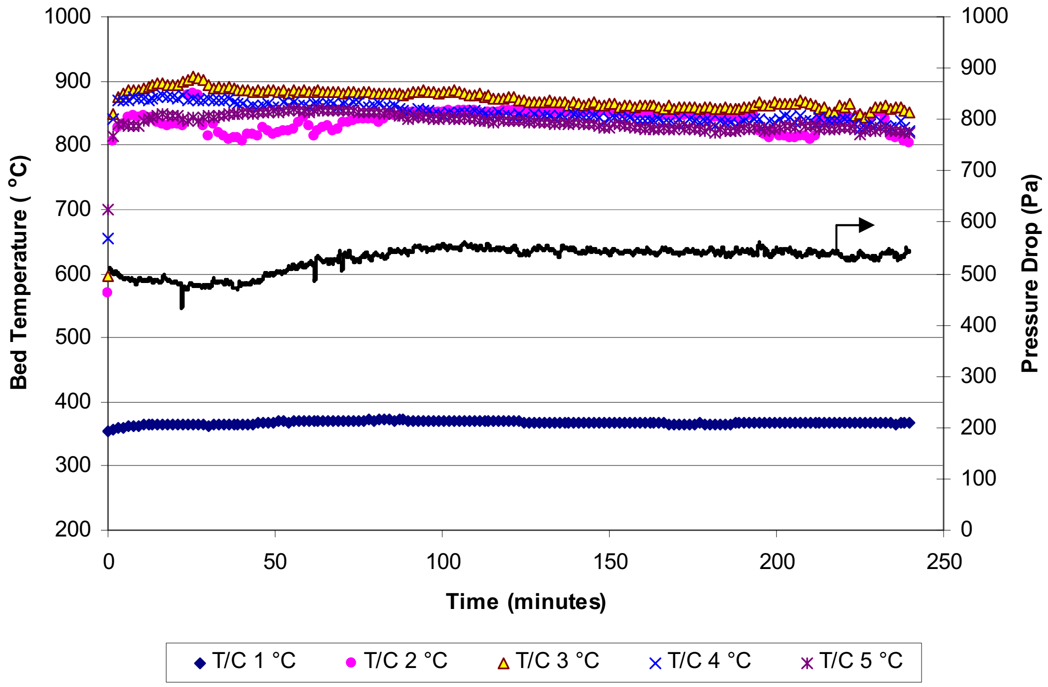

Figure B.15. Temperature and pressure drop profiles for Run B10.

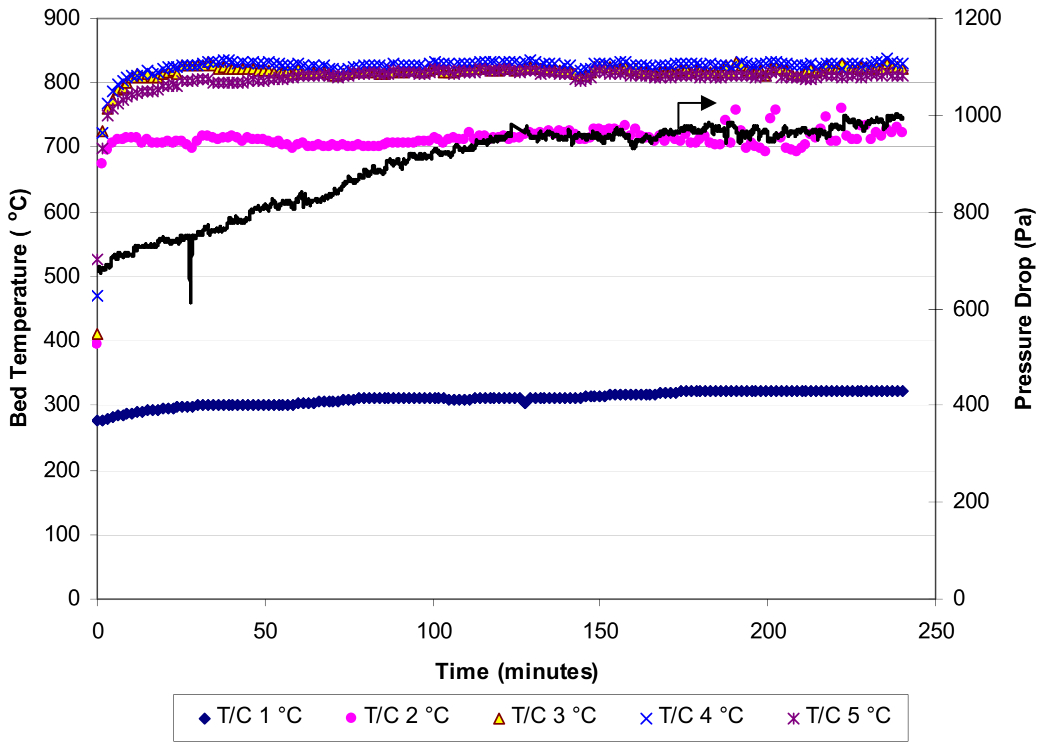

Figure B.16. Temperature and pressure drop profiles for Run B11.

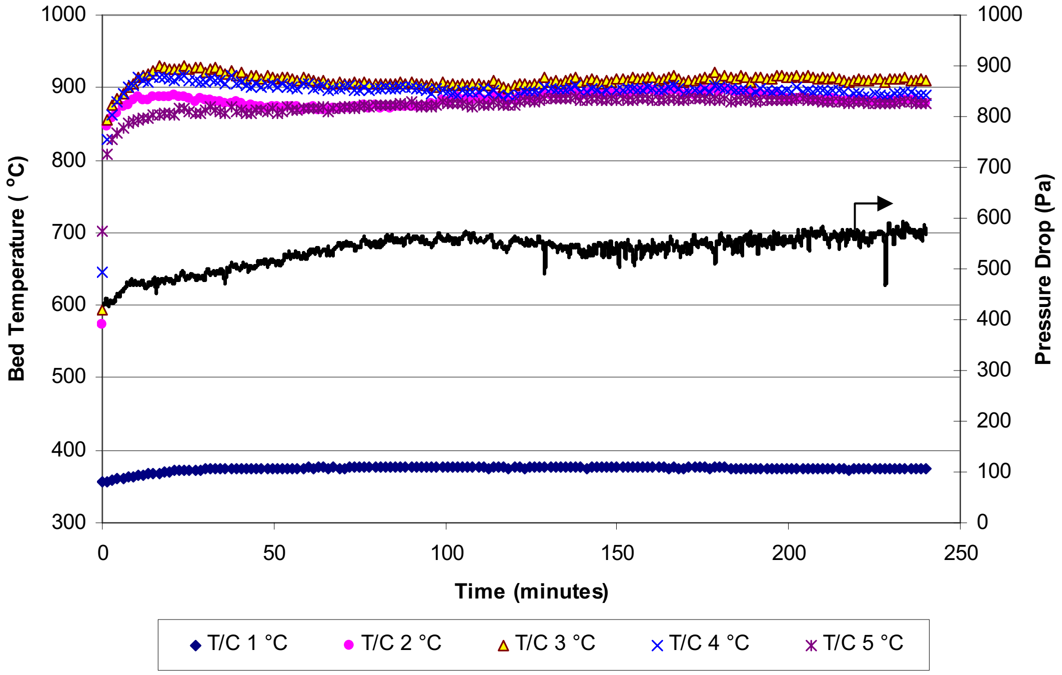

Figure B.17. Temperature and pressure drop profiles for Run B12.

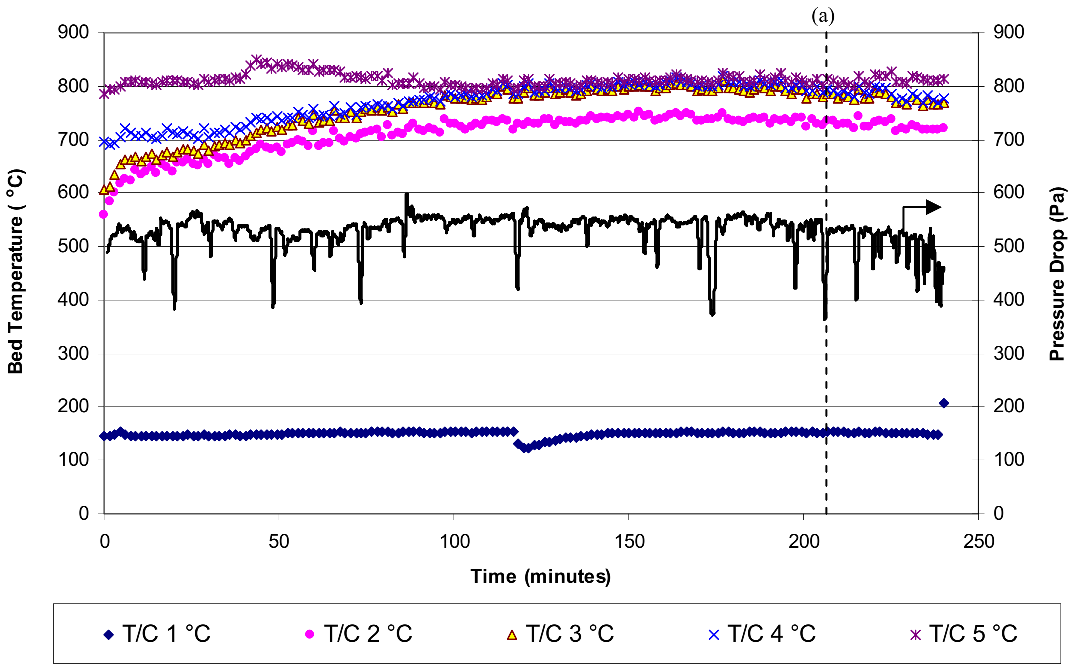

Figure B.18. Temperature and pressure drop profiles for Run C01. Apparent onset of defluidisation indicated by dashed line (a).

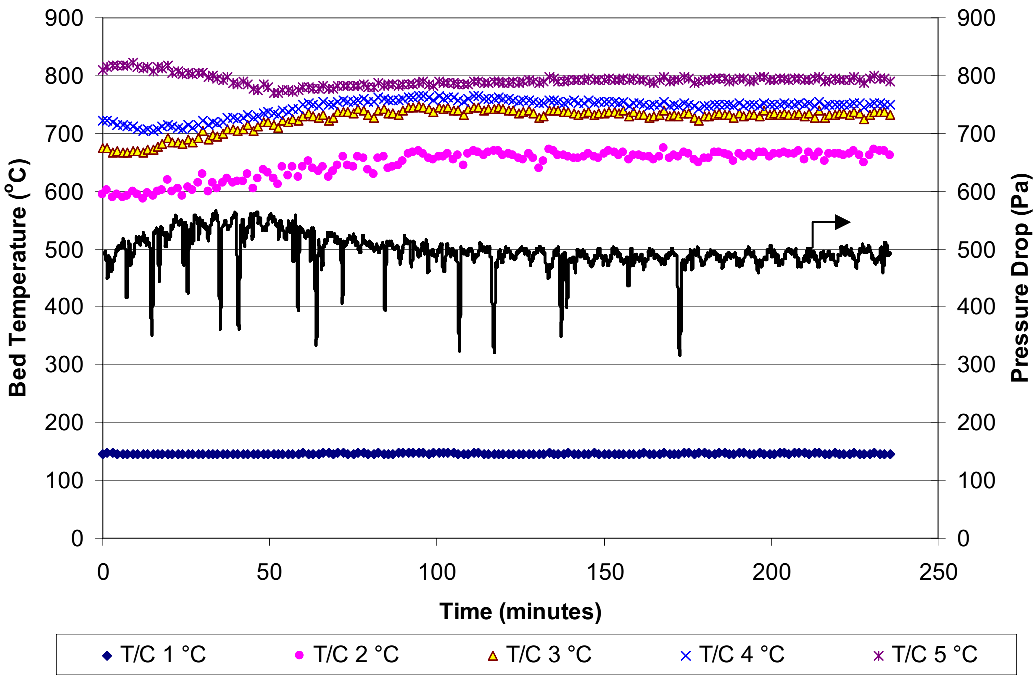

Figure B.19. Temperature and pressure drop profiles for Run C02.

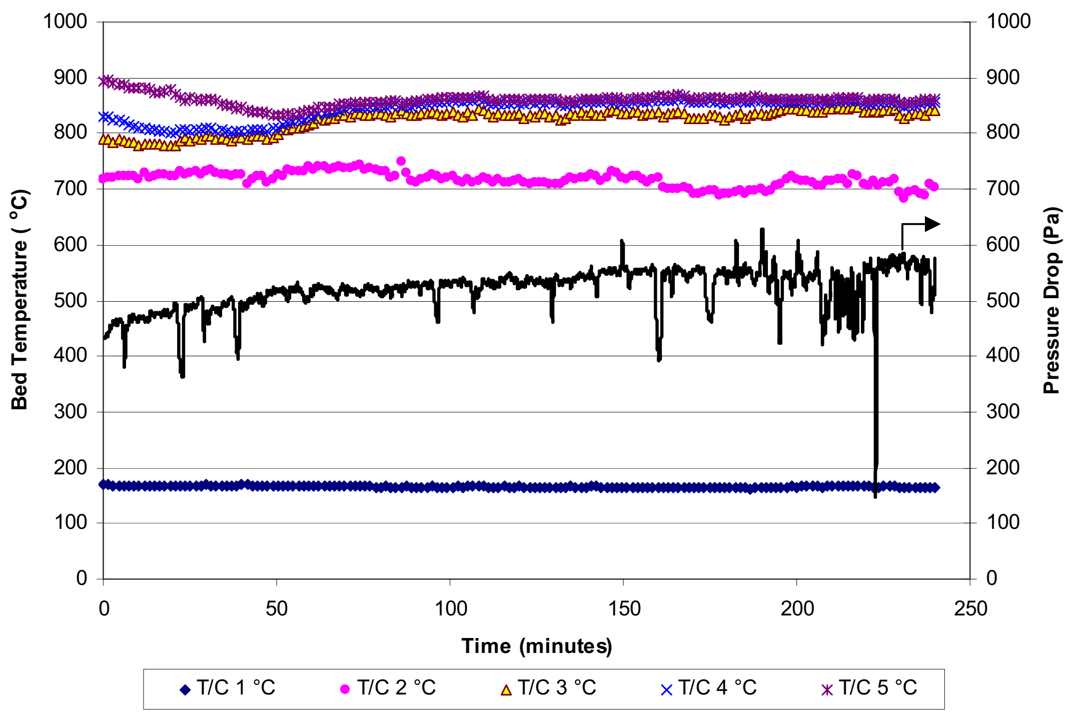

Figure B.20. Temperature and pressure drop profiles for Run C03.

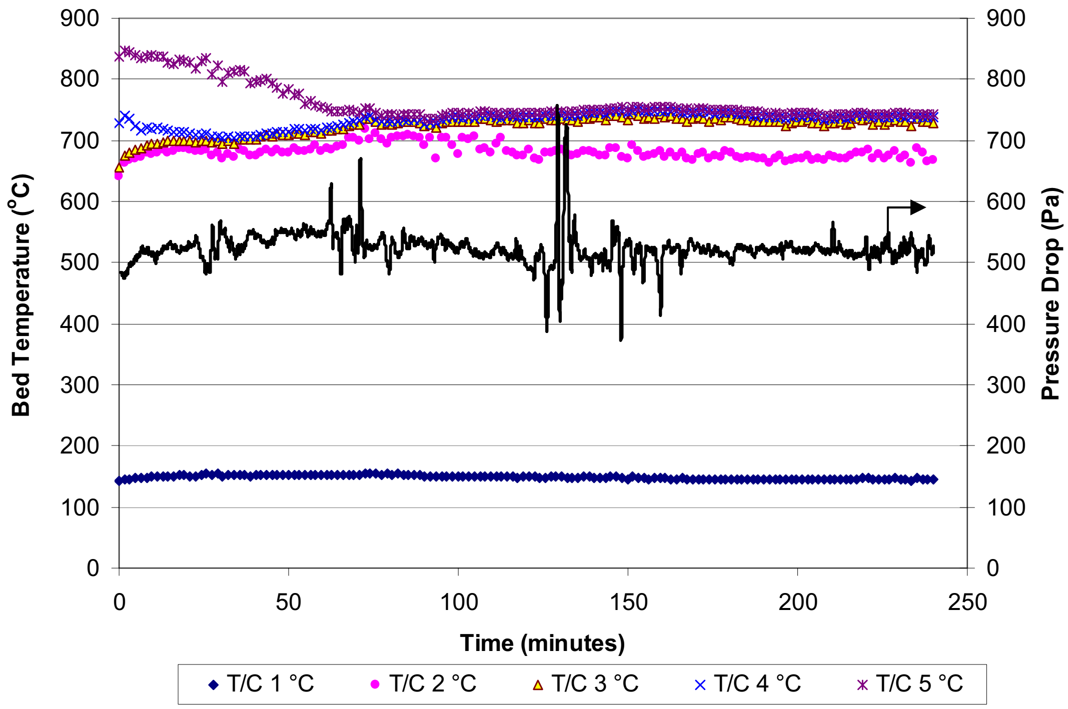

Figure B.21. Temperature and pressure drop profiles for Run C04.

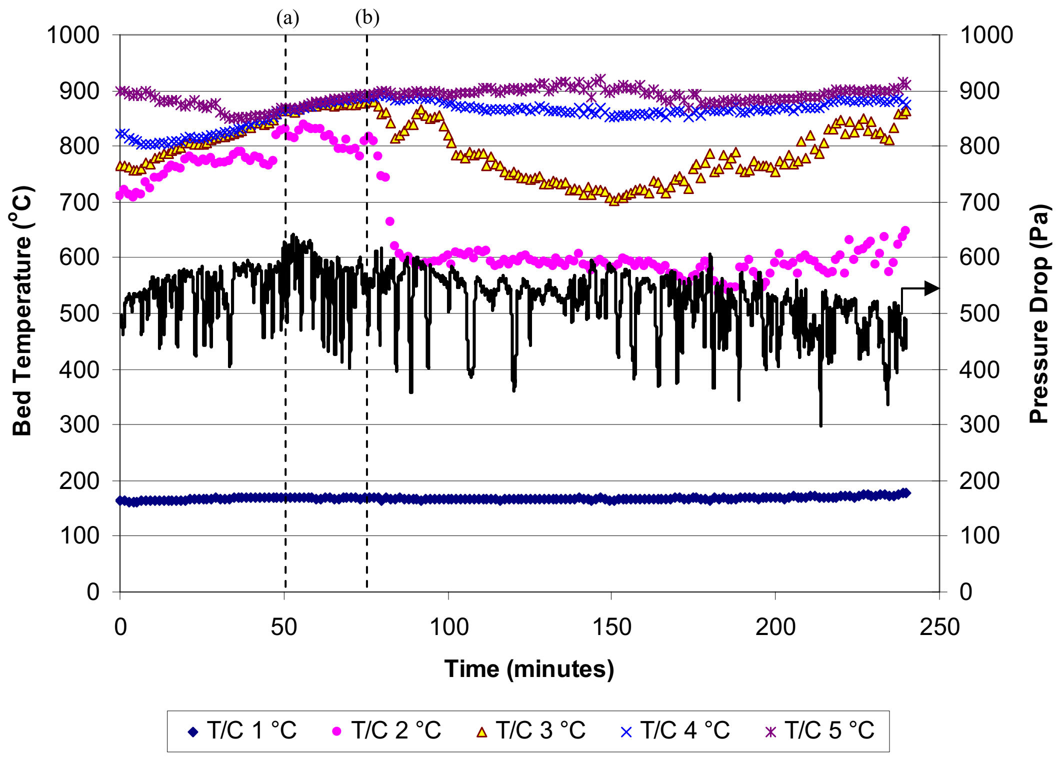

Figure B.22. Temperature and pressure drop profiles for Run C05. Operating range for apparent onset of defluidisation indicated by dashed lines (a) and (b).

APPENDIX C

ASH PARTICLES AND AGGOMERATES FROM FLUIDISED BED GASIFICATION EXPERIMENTS

C.1 Coated Mineral Particles

Figure C.1. Discrete bed particles retained on 3.35 mm sieve from Run A01.

Figure C.2. Discrete bed particles retained on 3.35 mm sieve from Run A02.

Figure C.3. Discrete bed particles retained on 3.35 mm sieve from Run A03.

Figure C.4. Discrete bed particles retained on 3.35 mm sieve from Run A04.

Figure C.5. Discrete bed particles retained on 3.35 mm sieve from Run A05.

Figure C.6. Discrete bed particles retained on 3.35 mm sieve from Run A06.

Figure C.7. Discrete bed particles retained on 3.35 mm sieve from Run B01.

Figure C.8. Discrete bed particles retained on 3.35 mm sieve from Run B02.

Figure C.9. Discrete bed particles retained on 3.35 mm sieve from Run B03.

Figure C.10. Discrete bed particles retained on 3.35 mm sieve from Run B05.

Figure C.11. Discrete bed particles retained on 3.35 mm sieve from Run B06.

Figure C.12. Discrete bed particles retained on 3.35 mm sieve from Run B07.

Figure C.13. Discrete bed particles retained on 3.35 mm sieve from Run B08.

Figure C.14. Discrete bed particles retained on 3.35 mm sieve from Run B11.

Figure C.15. Discrete bed particles retained on 3.35 mm sieve from Run B12.

C.2 Agglomerated Ash

Figure C.16. Agglomerated ash from Run A02.

Figure C.17. Agglomerated ash from Run A03.

Figure C.18. Agglomerated ash from Run A04.

Figure C.19. Agglomerated ash from Run A05.

Figure C.20. Agglomerated ash from Run A06.

Figure C.21. Agglomerated ash from Run B02.

Figure C.22. Agglomerated ash from Run B05.

Figure C.23. Agglomerated ash from Run B08.

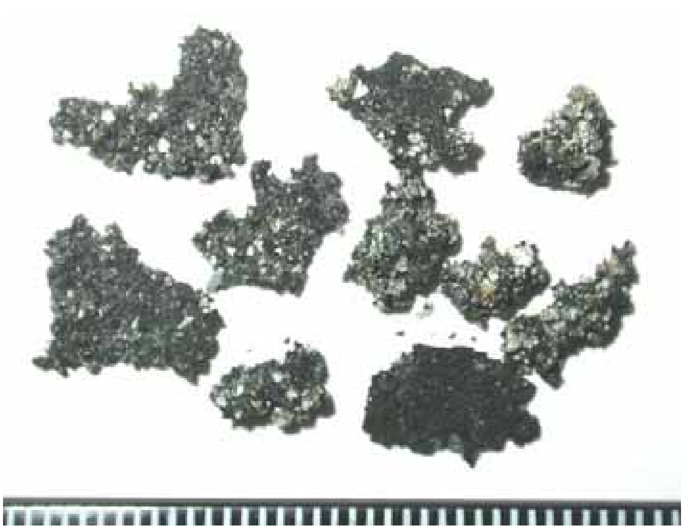

Figure C.24. Agglomerated ash from Run C01.

Figure C.25. Agglomerated ash from Run C02.

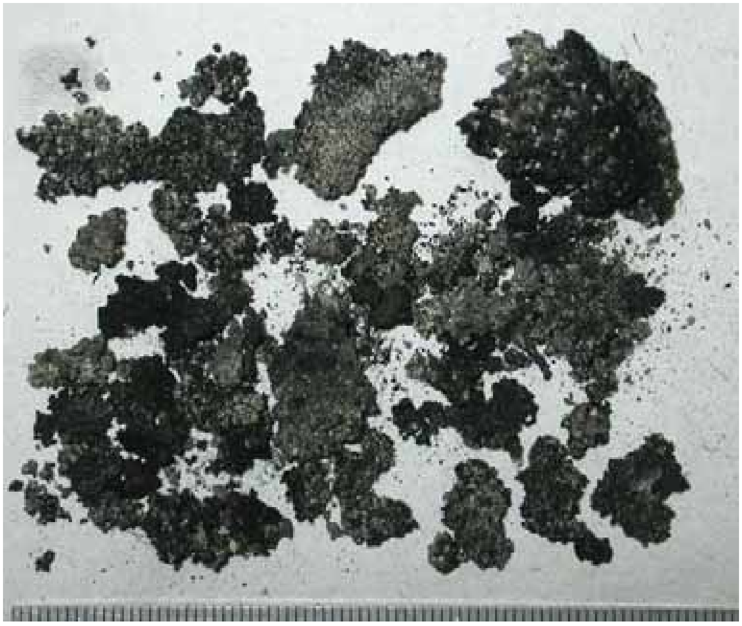

Figure C.26. Agglomerated ash from Run C03.

Figure C.27. Agglomerated ash from Run C04.

Figure C.28. Agglomerated ash from Run C05.

Figure C.29. Agglomerated ash from PDU tests.

APPENDIX D

INORGANIC ANALYSES OF FLUIDISED BED GASIFICATION SAMPLES

D.1 Elemental Analysis of Bed Char

Table D.1. Major elements detected via X-ray fluorescence analysis in bed char samples from spouted bed gasification experiments.

Run	SiO2 %	Al2O3 %	MgO %	Fe2O3 %	CaO %	Na2O %	K2O %	TiO2 %	P2O5 %	MnO %	SO3 %
B01	13.06	2.83	3.64	1.67	6.01	3.73	0.13	0.47	0.02	0.03	10.93
B02	36.75	7.06	9.11	6.7	13.49	7.62	0.21	1.17	0.04	0.1	6.34
B03	53.34	6.20	6.39	4.57	11.01	9.26	0.15	1.26	0.03	0.06	4.87
B05	40.46	5.76	5.8	5.54	12.82	7.49	0.15	0.87	0.04	0.06	9.51
B06	22.10	3.30	3.48	2.03	7.06	4.25	0.15	0.53	0.02	0.02	11.80
B07	26.62	3.46	3.55	3.04	8.90	4.71	0.15	0.58	0.02	0.02	13.50
B08	45.26	6.61	7.84	4.59	15.93	8.32	0.15	1.17	0.04	0.07	5.94
B09	23.25	2.78	3.19	3.18	7.17	3.88	0.12	0.44	0.03	0.02	13.55
B10	25.44	3.82	4.75	2.92	8.81	4.95	0.16	0.5	0.03	0.03	13.05
B11	31.72	5.21	6.55	4.09	12.19	5.09	0.13	0.6	0.04	0.04	15.36
B12	30.79	6.52	9.04	4.97	14.99	6.15	0.11	0.75	0.04	0.05	9.70
A01	36.17	5.95	6.74	3.57	12.92	6.44	0.15	0.76	0.03	0.05	7.97
A02	37.11	6.87	8.04	3.96	16.04	6.97	0.14	0.78	0.04	0.05	7.13
A03	35.76	7.11	9.07	6.67	15.77	7.61	0.14	1.11	0.04	0.10	8.74
A04	31.28	6.18	7.83	7.57	12.78	7.12	0.16	0.96	0.04	0.10	9.45
A05	46.89	7.41	8.88	4.33	16.23	8.87	0.15	1.23	0.04	0.06	1.24
A06	42.26	6.61	7.94	4.91	13.62	8.04	0.16	1.16	0.04	0.07	6.17
C01	23.86	4.53	5.34	3.27	8.44	4.54	0.15	0.59	0.03	0.04	9.30
C02	33.93	4.10	4.68	5.53	9.36	5.91	0.16	0.60	0.03	0.05	9.00
C03	32.71	5.46	5.86	5.18	10.34	5.81	0.16	0.72	0.04	0.07	10.21
C04	17.23	4.65	6.18	2.46	7.63	4.72	0.15	0.59	0.03	0.05	7.04
C05	29.33	6.61	8.34	7.87	13.91	6.70	0.14	0.77	0.04	0.07	12.49

Table D.2. Trace elements detected via X-ray fluorescence analysis in bed char samples from spouted bed gasification experiments.

Run	ZnO ppm	CuO ppm	SrO ppm	ZrO2 ppm	NiO ppm	Rb2O ppm	BaO ppm	V2O5 ppm	Cr2O3 ppm	La2O3 ppm
B01	19	40	536	160	22	7	602	31	15	29
B02	71	53	1301	311	1772	11	1043	79	1849	46
B03	56	24	1089	342	975	9	1653	78	522	42
B05	97	103	1005	235	1570	8	3197	61	5430	17
B06	12	32	546	156	74	6	1157	30	332	14
B07	20	24	593	143	40	3	1164	45	256	25
B08	71	48	1320	320	1111	8	1365	68	2672	28
B09	23	94	511	135	547	10	586	37	1910	2
B10	25	70	728	156	126	8	1292	40	369	10
B11	19	80	970	141	63	6	1230	43	325	7
B12	31	35	1389	125	626	0	5188	54	2510	50
A01	19.3	30.4	1032	193	662	1	318	49	530	32
A02	20	25	1386	181	541	1	5450	59	540	42
A03	31.9	30.5	1373	248	2531	0	1567	82	7171	55
A04	27	51.7	1141	207	4941	2	1086	96	12181	52
A05	35	32.6	1423	286	923	3	1402	59	2164	49
A06	36.2	32.4	1264	274	1316	3	4141	59	1847	49
C01	39	79	740	280	490	3	358	43	1095	29
C02	36	67	699	140	1381	1	1138	49	2110	40
C03	16	73	851	257	1605	5	377	60	2040	36
C04	17	61	818	266	122	11	450	34	265	30
C05	91.8	55.1	1145	184	2271	0	503	55	4690	85

Run	CeO2 ppm	PbO ppm	Y2O3 ppm	CoO ppm	Ga2O3 ppm	U3O8 ppm	ThO2 ppm	As2O5 ppm	SnO2 ppm	Cl ppm
B01	15	19	8	23	3	16	6	9	0	5558
B02	71	20	31	107	10	22	-11	17	-4	2206
B03	52	27	21	50	6	17	0	16	1	2951
B05	42	30	17	71	9	21	-11	15	29	4748
B06	18	0	10	32	2	13	0	5	0	7760
B07	16	4	6	53	1	6	0	5	1	7254
B08	54	16	24	55	5	24	-13	15	-1	3339
B09	9	1	7	103	5	23	10	1	-3	7539
B10	31	2	10	122	7	25	8	7	-3	6184
B11	32	5	10	94	5	16	-4	8	-2	6456
B12	41	17	15	21	2	0	0	24	3	2622
A01	41	13	17	15	3	0	0	18	0	1645
A02	38	14	17	13	4	0	0	23	1	1846
A03	80	18	21	25	3	0	0	25	0	2431
A04	63	14	16	29	6	0	0	28	2	4213
A05	57	17	26	17	5	0	0	28	0	1073
A06	48	15	20	19	3	0	0	24	0	1895
C01	20	0	10	13	0	0	0	18	0	2376
C02	41	4	8	16	2	0	0	21	4	2529
C03	49	9	13	19	4	0	0	21	17	998
C04	23	0	21	11	6	16	20	21	0	4636
C05	53	3	18	37	5	0	0	31	6	1247

D.2 Elemental Analysis of Agglomerate Samples

Table D.3. Major elements detected via X-ray fluorescence analysis in agglomerate samples from spouted bed gasification experiments.

Runs	SiO2 %	Al2O3 %	MgO %	Fe2O3 %	CaO %	Na2O %	K2O %	TiO2 %	P2O5 %	MnO %	SO3 %
B02	46.34	8.24	10.18	6.75	14.84	9.39	0.26	1.37	0.07	0.11	3.65
B05	51.42	6.29	7.58	5.87	13.71	10.21	0.16	1.41	0.04	0.08	3.61
B08	49.83	7.28	8.39	4.45	16.72	9.02	0.15	1.31	0.04	0.07	3.20
A03	47.24	8.18	10.39	6.27	16.49	8.60	0.17	1.38	0.05	0.11	2.63
A04	45.62	8.22	10.42	6.45	16.40	9.23	0.17	1.38	0.05	0.12	2.65
A05	48.72	8.00	9.89	4.64	15.41	9.33	0.15	1.21	0.05	0.07	1.16
A06	48.22	7.69	9.78	5.37	15.74	9.19	0.16	1.43	0.05	0.08	2.84
C01	52.54	5.21	4.90	10.44	12.42	11.36	0.21	0.72	0.03	0.11	3.94
C02	53.36	4.64	3.73	14.87	10.80	10.91	0.26	0.59	0.03	0.13	2.70
C03	60.68	3.83	1.95	10.11	8.57	9.25	0.19	0.26	0.01	0.03	5.14
C05	53.18	4.93	4.60	6.97	11.25	10.68	0.23	0.70	0.02	0.05	7.45

Table D.4. Trace elements detected via X-ray fluorescence analysis in agglomerate samples from spouted bed gasification experiments.

Run	ZnO ppm	CuO ppm	SrO ppm	ZrO2 ppm	NiO ppm	Rb2O ppm	BaO ppm	V2O5 ppm	Cr2O3 ppm	La2O3 ppm
B02	30	44	1491	368	1413	13	1002	76	566	45
B05	57	13	1250	389	986	5	1374	83	4146	50
B08	40	11	1408	368	597	7	1542	69	1040	54
A03	19.9	27.8	1534	415.4	722.8	10.3	1174.1	77.3	1524.3	50.4
A04	22.5	33.2	1560.1	411.1	969.4	10.8	989	69.3	1327.2	46.3
A05	38.6	24.9	1781.4	345.8	1037.9	14.9	10542	74.2	2498.5	48.4
A06	32.2	30.8	1505.4	398.2	1116.9	9.5	1656.6	67.6	1042.1	48.7
C01	28	59	843	528	4722	24	885	79	6841	77
C02	10	65	672	358	8570	28	1553	106	9738	65
C03	31	26	451	141	708	10	1207	38	560	41
C05	41	27	785	210	405	9	1535	46	425	44

Run	CeO2 ppm	PbO ppm	Y2O3 ppm	CoO ppm	Ga2O3 ppm	U3O8 ppm	ThO2 ppm	As2O5 ppm	SnO2 ppm	Cl ppm
B02	70	24	37	28	6	26	-13	18	-7	382
B05	67	18	31	65	8	20	0	16	0	1979
B08	64	22	33	54	5	20	0	20	0	1320
A03	51.6	21.9	41.9	20.2	12.7	21.5	4.2	18.8	0	351.2
A04	64.6	19.5	34.7	25	11.3	14.5	0	21	0	410
A05	57.9	23.5	39.9	12.7	14	12.9	7.4	19.7	0	629.9
A06	40	19.5	37.6	24	12.4	15.2	2.3	19	0	681.7
C01	49	0	43	48	28	55	33	16	0	1134
C02	57	0	38	46	39	72	41	12	0	563
C03	24	1	15	12	10	23	0	10	0	920
C05	29	0	16	7	13	0	0	24	4	695

D.3 Elemental Analysis of Cyclone Dust Samples

Table D.5. Major elements detected via X-ray fluorescence analysis in cyclone dust samples from spouted bed gasification experiments.

Run	SiO2 %	Al2O3 %	MgO %	Fe2O3 %	CaO %	Na2O %	K2O %	TiO2 %	P2O5 %	MnO %	SO3 %
B01	8.97	4.15	5.60	2.84	7.82	4.01	0.13	0.44	0.03	0.08	11.84
B02	7.08	5.71	7.86	3.32	9.8	3.54	0.12	0.45	0.04	0.1	10.54
B03	8.70	4.28	6.15	3.18	8.33	3.73	0.12	0.46	0.03	0.08	12.20
B05	7.47	4.64	6.48	3.25	8.34	3.16	0.11	0.43	0.03	0.08	11.18
B06	7.04	3.27	4.57	2.11	5.77	3.79	0.12	0.36	0.03	0.05	11.89
B07	8.60	3.70	5.00	2.60	6.81	3.96	0.13	0.41	0.03	0.07	11.17
B08	9.74	5.34	7.19	3.92	9.91	3.39	0.11	0.52	0.04	0.09	12.82
B09	8.6	3.46	4.42	2.61	7.33	4.12	0.12	0.36	0.03	0.08	12.96
B10	10.52	4.53	5.99	3.44	9.07	4.68	0.14	0.56	0.03	0.09	13.48
B11	11.99	5.04	6.66	3.43	9.96	4.97	0.13	0.55	0.03	0.1	13.7
B12	9.86	5.35	7.27	4.41	10.11	3.91	0.10	0.54	0.04	0.10	11.72
A01	11.78	5.90	8.13	4.38	10.89	4.13	0.13	0.66	0.04	0.10	13.07
A02	11.23	5.71	8.00	3.99	10.56	4.06	0.12	0.64	0.04	0.10	12.74
A03	9.58	5.62	7.71	4.60	10.52	3.96	0.11	0.55	0.04	0.11	13.07
A04	8.55	4.87	6.70	4.17	9.38	3.75	0.11	0.44	0.04	0.09	12.42
A05	12.58	6.42	8.91	5.24	12.15	4.28	0.11	0.66	0.05	0.12	12.49
A06	9.61	6.25	8.63	4.17	11.60	3.59	0.11	0.54	0.04	0.10	12.07
C01	9.16	5.04	7.00	4.19	9.32	3.61	0.10	0.46	0.03	0.09	8.25
C02	7.97	4.76	6.66	3.80	8.90	3.41	0.10	0.39	0.03	0.08	7.37
C03	7.70	4.66	6.33	3.25	8.88	3.20	0.10	0.39	0.03	0.08	8.31
C04	7.37	4.33	5.51	3.46	8.55	2.85	0.09	0.38	0.03	0.09	8.18
C05	9.71	6.17	8.76	3.34	10.93	4.58	0.13	0.60	0.04	0.11	7.04

Table D.6. Trace elements detected via X-ray fluorescence analysis in cyclone dust samples from spouted bed gasification experiments.

Run	ZnO ppm	CuO ppm	SrO ppm	ZrO2 ppm	NiO ppm	Rb2O ppm	BaO ppm	V2O5 ppm	Cr2O3 ppm	La2O3 ppm
B01	25	30	806	138	472	5	427	30	108	21
B02	30	49	1081	150	933	10	402	46	128	36
B03	12	42	851	133	1433	5	332	37	337	25
B05	17	27	891	138	557	3	327	39	683	24
B06	17	45	643	129	462	7	241	29	289	13
B07	18	25	718	127	152	5	379	29	186	22
B08	13	24	997	127	255	0	389	33	261	28
B09	24	59	665	111	595	6	368	28	853	25
B10	23	34	884	153	230	7	568	36	247	30
B11	21	41	995	154	92	4	504	41	109	30
B12	24	47	1017	152	1659	4	419	43	468	23
A01	18	45	1111	170	580	3	479	50	456	21
A02	20	51	1076	163	586	4	479	45	278	26
A03	24	74	1057	143	1585	3	487	44	2369	27
A04	17	66	916	122	1607	4	373	37	1673	19
A05	21	47	1207	177	1095	2	639	49	1824	26
A06	15	46	1184	144	705	5	509	44	249	25
C01	30	74	961	159	1298	4	385	42	2721	33
C02	21	55	935	129	1228	6	395	45	2988	36
C03	23	50	910	141	583	5	357	35	971	29
C04	14	42	814	141	494	6	373	27	783	22
C05	28	23	1218	183	293	10	409	39	441	49

Run	CeO2 ppm	PbO ppm	Y2O3 ppm	CoO ppm	Ga2O3 ppm	U3O8 ppm	ThO2 ppm	As2O5 ppm	SnO2 ppm	Cl ppm
B01	25	7	12	17	1	4	0	12	1	11646
B02	35	13	16	397	4	15	7	22	0	12168
B03	17	3	12	19	2	3	0	16	4	10498
B05	25	7	11	19	1	1	0	18	6	10505
B06	10	0	10	14	2	13	8	8	0	11679
B07	9	5	5	12	1	2	0	12	4	11437
B08	29	4	9	22	0	0	0	16	2	8243
B09	19	7	6	18	2	6	-2	9	1	13056
B10	29	14	7	17	0	0	-10	14	8	13057
B11	24	14	10	20	1	0	-10	15	3	14709
B12	27	6	16	24	5	0	3	23	2	9076
A01	36	8	16	20	4	0	0	29	3	6662
A02	27	12	17	20	6	0	1	26	2	7081
A03	26	9	16	28	5	0	0	26	5	8829
A04	17	7	13	21	5	0	1	22	1	7617
A05	30	11	17	28	4	0	0	29	2	8819
A06	22	6	16	20	5	0	2	31	0	7956
C01	32	0	14	27	4	0	0	22	0	8479
C02	26	7	15	18	5	0	0	21	0	7199
C03	27	0	15	20	2	0	2	20	0	6897
C04	32	2	13	18	5	0	3	19	0	6467
C05	37	7	22	19	8	0	9	29	7	13710

D.4 Elemental Analysis of Inlet Deposit Samples

Table D.7. Major elements detected via X-ray fluorescence analysis in inlet deposit samples from spouted bed gasification experiments.

Run	SiO2 %	Al2O3 %	MgO %	Fe2O3 %	CaO %	Na2O %	K2O %	TiO2 %	P2O5 %	MnO %	SO3 %
NSB01	6.53	8.85	13.71	4.60	14.42	15.27	0.40	0.66	0.07	0.07	29.75
NSB02	9.81	4.49	5.57	4.18	8.48	22	0.68	0.37	0.08	0.06	37.89
NSB03	5.09	6.34	10.24	3.71	11.95	21.36	0.43	0.48	0.05	0.07	38.90
NSB05	5.87	6.98	11.01	3.99	11.86	19.97	0.48	0.48	0.05	0.07	37.16
NSB06	6.39	8.75	13.81	4.76	14.67	15.35	0.39	0.80	0.07	0.08	30.44
NSB07	8.52	6.04	9.13	4.64	11.27	20.20	0.44	0.52	0.07	0.06	33.87
NSB08	7.17	7.71	11.70	4.00	12.63	18.17	0.57	0.54	0.05	0.06	37.29
NSB09	6.05	7.11	10.07	4.05	11.44	19.09	0.47	0.52	0.08	0.05	32.75
NSB10	21.82	6.61	9.13	6.25	11.93	14.03	0.38	0.55	0.05	0.07	26.53
NSB11	6.45	7.59	11.17	4.14	12.61	15.38	0.34	0.53	0.09	0.06	31.11
NSB12	8.85	5.46	8.18	4.37	9.76	20.28	0.90	0.42	0.05	0.05	38.16
AF01	6.66	7.91	11.16	5.19	11.22	14.75	0.67	0.61	0.06	0.06	33.31
AF02	12.20	6.40	8.39	7.77	10.07	15.56	0.30	0.48	0.07	0.09	23.56
AF03	11.34	5.35	7.74	6.80	9.84	19.46	0.58	0.41	0.04	0.07	34.23
AF04	6.74	4.49	6.56	6.73	8.22	20.08	0.69	0.33	0.05	0.06	37.37
AF05	16.03	6.18	9.18	5.37	12.16	14.62	0.44	0.45	0.05	0.07	32.09
AF06	10.36	5.60	8.41	4.28	9.91	21.12	0.72	0.38	0.05	0.05	36.07

Table D.8. Trace elements detected via X-ray fluorescence analysis in inlet deposit samples from spouted bed gasification experiments.

Run	ZnO ppm	CuO ppm	SrO ppm	ZrO2 ppm	NiO ppm	Rb2O ppm	BaO ppm	V2O5 ppm	Cr2O3 ppm	La2O3 ppm
B01	37	187	1705	312	1393	23	572	64	1998	52
B02	141	1904	1068	1362	1606	143	2612	61	2211	-114
B03	34	229	1369	150	1887	8	627	60	2133	30
B05	52	181	1405	174	1025	8	759	53	3994	17
B06	64	235	1648	512	445	42	623	82	1310	65
B07	62	251	1401	630	1228	58	849	56	4140	72
B08	36	128	1425	153	587	6	606	50	1641	18
B09	55	385	1348	702	937	75	818	43	2726	23
B10	36	226	1254	258	2238	23	1201	66	4877	27
B11	54	457	1373	774	311	93	796	69	667	-62
B12	57	465	1072	283	2342	38	657	37	3818	0
A01	26	427	1288	290	2376	39	493	38	3033	14
A02	76	456	1068	705	5628	78	834	81	12756	13
A03	37	345	1036	224	3121	15	1025	54	13483	19
A04	41	323	2153	184	2959	26	44888	91	10054	11
A05	39	215	1237	203	2913	9	2316	72	16887	27
A06	53	398	1114	319	1250	35	1280	50	5187	0

Run	CeO2 ppm	PbO ppm	Y2O3 ppm	CoO ppm	Ga2O3 ppm	U3O8 ppm	ThO2 ppm	As2O5 ppm	SnO2 ppm	Cl ppm
B01	47	10	40	34	13	67	47	0	0	31770
B02	-19	-118	125	-1	74	493	371	-106	-159	1846
B03	13	2	7	26	5	18	0	7	12	6185
B05	5	2	7	27	0	21	0	4	26	4616
B06	53	0	56	22	13	138	110	0	0	27932
B07	6	68	70	25	32	202	154	0	0	32981
B08	25	4	8	18	0	14	0	3	10	1576
B09	-18	-9	63	24	33	244	220	-52	-52	40538
B10	44	15	21	25	9	60	24	-6	1	11551
B11	20	-32	60	15	40	309	234	-82	-109	11631
B12	0	0	31	24	21	53	101	6	0	1077
A01	0	0	33	21	20	43	81	3	0	6678
A02	0	0	76	45	69	162	238	13	0	36935
A03	10	13	13	32	16	13	26	16	17	2183
A04	0	0	11	26	25	10	25	16	0	1135
A05	2	9	9	31	10	0	0	13	10	1269
A06	0	0	34	12	26	65	106	23	0	2012